# Modeling of Water/n- Alkane Mixtures with SAFT - VR-SW and SAFT-γ-Mie GC approach EoS

**Rita Patrício Gomes**

Thesis to obtain the Master of Science Degree in

## Chemical Engineering

Supervisors: Prof. Dr. Eduardo Morilla Filipe

Prof. Dr. Amparo Galindo

## Examination Committee

Chairperson: Prof Dr. Maria Norberta Correia de Pinho

Supervisors: Prof. Dr. Eduardo Morilla Filipe

Member of the Committee: Dr. Pedro Jorge Rodrigues Morgado

**December 2014**

*“Experience is simply the name we give our mistakes.”*

Oscar Wilde

# Acknowledgements

No piece of work is the sole result of a one person's effort, and this one would not have been done without the help and support of not only Professors but also friends and family. First I have to thank Dr. Eduardo Jorge Morilla Filipe, my supervisor, who not only introduced me to this theme, but supported and encouraged me every step of the way, along with Dr. Amparo Galindo, my supervisor at Imperial College for all the insight and support throughout my stay in London. I also want to thank Dr. Pedro Morgado who was always present to help me with all sorts of problems and always presented me with new ideas, along with the research group at the Molecular Systems engineering who made me feel very welcome and whose suggestions and questions allowed me to make a much better job.

I would like to express my profound gratitude to my family, specially my mother and sister for always believing and supporting me in all possible ways, without you this thesis would not have been finished.

I want to thank all my friends, for listening and accompanying me since the beginning of this journey, especially Bernardo Barros and Catia Lopo. I owe a special thank you to João Pedro who accompanied me in a daily basis although we were miles apart, always with a friendly and wise word, to José Pereira for his unconditional support, for inspiring and pushing me to always give my best, and of course to Rafael Santos who is my most faithful friend and supporter, who guides me and has a way of always showing me what I am yet to realize is best.

# Resumo

As misturas de água/n-alcanos ocupam um importante lugar na realidade energética de hoje, onde a fonte de energia mais utilizada continua a ser o petróleo. Dada a importância de prever as propriedades termodinâmicas deste tipo de sistemas, duas versões da Statistical Associating Fluid Theory (SAFT) foram utilizadas para a prever a solubilidade e funções termodinâmicas dos sistemas água/n-hexano, água/n-heptano, água/n-undecano e água/n-hexadecano. Utilizou-se a teoria SAFT-VR-SW, onde as moléculas são modeladas como cadeias de monómeros esféricos tangentes, com potencial intermolecular do tipo fosso quadrado. O parâmetro de interacção binário, $K_{ij}$, foi ajustado à composição da fase orgânica de cada sistema, o que conduziu a uma melhor concordância entre as curvas de solubilidade teóricas e os resultados experimentais. Foi também utilizada a SAFT-γ-Mie para a descrição dos sistemas em estudo. Esta versão da teoria foi desenvolvida como um método de contribuição de grupos, onde as moléculas são modeladas por cadeias heteronucleares de esferas fundidas representando os distintos grupos funcionais. As interacções entre segmentos são descritas por um potencial Mie. Esta abordagem apresentou as melhores previsões da solubilidade mútua dos sistemas estudados. Com os dados de solubilidade na fase orgânica obtidos com ambas as versões da teoria, calcularam-se ainda as funções termodinâmicas de solução $\Delta_{sol}H_m^0$, $\Delta_{sol}S_m^0$, $\Delta_{svt}H_m^0$ e $\Delta_{svt}S_m^0$. Verificou-se que as funções termodinâmicas obtidas a partir das previsões de ambas as teorias, SAFT-VR-SW e SAFT-γ-Mie, conseguem traduzir os resultados experimentais, embora estes apresentem uma variação mais acentuada com o aumento da cadeia do alcano.

# Abstract

The water/n-alkane mixtures are very important for the reality we live in, where the most used source of energy is petroleum. Given the importance of predicting the thermodynamic properties of this type of systems, two approaches of the Statistical Associating Fluid Theory (SAFT) were used to predict the mutual solubility, and the thermodynamic functions of the water/n-hexane, water/n-heptane, water/n-undecane and water/n-hexadecane system. The SAFT-VR-SW theory was used, where molecules are modeled as chains of spherical segments with attractive forces represented with the square-well potential. In this approach a binary interaction parameter, $K_{ij}$, was fitted for each system, in the oil rich phase. The solubility curves obtained were a much better prediction of the experimental data than those obtained with no fitted $K_{ij}$. The SAFT-γ-Mie approach was also used to describe the water/n-alkane systems. SAFT-γ-Mie is formulated within the framework of a group contribution approach, where molecules are represented as chains of heteronuclear fused spheres comprising distinct functional chemical groups, where interaction between segments are described with the Mie potential of variable attractive and repulsive range. This approach presented the best results in the prediction of the mutual solubility of the studied systems. With the solubility results of the oil-rich phase obtained with both theories, the thermodynamic functions of solution, $\Delta_{sol}H_m^0$, $\Delta_{sol}S_m^0$, and solvation, $\Delta_{svt}H_m^0$ and $\Delta_{svt}S_m^0$were also obtained. The results showed that the thermodynamic functions obtained from the predictions of both theories, SAFT-VR-SW and SAFT-γ-Mie are able to describe the experimental results, although these presented a more pronounced dependence with the chain length of the alkane.

# Contents

# List of tables

# List of figures

# Nomenclature

## Abbreviations

AAD average absolute deviation

EoS Equation of state

HS hard sphere

LJ Lennard-Jones Potential

GC Group contribution model

M monomer reference system

SAFT Statistical Associating fluid theory

VR Model type of the equation of state (variable range)

## Greek symbols

α van der Waals attractive parameter

$\epsilon$ Depth of pair potential, J

$\epsilon/k_B$ Energy of dispersive interaction, K

$\xi$ Binary interaction parameter

η Packing fraction

$\gamma$ Model type of the equation of state

$\gamma_{ij}$ Binary interaction parameter

$\Lambda$ de Broglie wavelength,

$\lambda^{att}$ Attractive exponent of the Mie Potential

$\lambda^{rep}$ Repulsive exponent of the Mie Potential

ρ Number density

σ Segment diameter, A°

## Roman symbols

$A$ Helmholtz free energy, J

$a_1$ Helmholtz free energy per monomer segments of first-order perturbation term, J

$a_2$ Helmholtz free energy per monomer segments of second-order perturbation term, J

$a_3$ Helmholtz free energy per monomer segments of third-order perturbation term, J

$c_{kl}$ prefactor

$d$ Effective hard-sphere diameter

*e* electron

*g (r)* radial distribution function

*H* hydrogen

*k* chemical functional group

$K_{ij}$ Binary interaction parameter

$k_B$ Boltzmann constant, J $K^{-1}$

$m$ Number of segments per chain

$N$ Total number of molecules.

$N_a$ Avogrado's number

$N_G$ number of types of groups present

$N_s$ Total number of spherical segments

S Shape factor

T Temperature K

$U$ intermolecular potential function

$v_k^*$. Number of segments

$X_a$ fraction of molecules not bonded at site *a*

$x_{s,k}$ fraction of segments of a group of type k in the mixture

$y$ $(\sigma)$ background correlation function

## Subscripts

*i* Denotes the spherical segment from the pure compound

*i; j* Denotes the unlike interactions between the spherical segments

*j* Denotes the spherical segment from the pure compound

*k* Denotes the spherical segment from a chemical functional group

*k;l* Denotes the unlike interactions between the spherical segments

*l* Denotes the spherical segment from a chemical functional group

## Superscripts

ASSOC Association contribution

Att Attractive parameter

CHAIN Contribution due to the formation of chains

HB Hydrogen Bond

HS hard sphere

IDEAL Contribution due to the ideal gas

M Monomer reference system

MIE intermolecular potential type

MONO Contribution of monomer system.

Rep Repulsive parameter

SW intermolecular potential type (squared well)

# Chapter 1

## Introduction

### 1.1 Water/n-alkanes interaction

It is of common knowledge that the world we live in needs an incredible amount of energy. Despite the efforts devoted to renewable and ecologically friendly sources of energy, petroleum continues to be the most important one. The operational costs of the extraction, transport, and transformation are increasing while the source amount is thought to be decreasing, (Ferguson, Debenedetti, & Panagiotopoulos, 2009). Therefore, is necessary to optimize the process through a better knowledge of the thermodynamic behavior of petroleum, which is, chemically, a complex mixture of hydrocarbons. Data concerning water-hydrocarbon systems are required for the design of a variety of chemical engineering separation operations, especially those concerned with water pollution abatement and petroleum extraction. Although these processes are performed at high temperatures and pressures nearly all available data are at ambient conditions, (Marche, Ferronato, & Jose, 2003). Given the need for a considerably quantity of data in a large spectrum of temperatures and pressure and in order to permit the optimization of the processes, it is necessary to find more accurate models to describe the mutual solubility and thermodynamic properties between these compounds.

Mixtures of water and hydrocarbons exhibit limited miscibility over a wide range of temperatures, thus giving rise to two distinct phases: A hydrocarbon - rich phase containing a very small concentration of water molecules and a water-rich phase, containing an even smaller concentration of dissolved hydrocarbon. Most of the published experimental data (Shaw, Maczynski, & Goral, 2005) indicates that the solubility of hydrocarbons in water is highly dependent on the hydrocarbon, with larger molecules being less soluble. On the other hand, the solubility of water in hydrocarbons depends much less on the hydrocarbon chain length.

Water-hydrocarbon mixtures are very non-ideal mixtures, since water and hydrocarbons are very different substances, engaging in different interactions with one another. For instance, between hydrocarbons, dispersive interactions prevail, while in the water rich phase, since water is a small polar molecule, capable of establishing strong hydrogen bonds, this type of interaction prevails.

When a hydrocarbon molecule is dissolved in water, a number of hydrogen bonds are broken depending on the size of the cavity needed to accommodate the hydrocarbon molecule, therefore, on the size and shape of the hydrocarbon. The water molecules around the hydrocarbon rearrange in order to maximize the formation of hydrogen bonds, this is known as hydrophobic effect. From this effect results a decrease of entropy since water molecules rearrange in order to be able to establish new hydrogen bonds, resulting in a more organized arrangement.

On the hydrocarbon rich phase, when water is dissolved, the situation is very different. Considering that first one has pure water and pure n-alkane, when water is added to the n-alkane in a very small proportion of water molecules/alkane molecules, all of the hydrogen bonds of the pure water are broken, and water molecules are isolated between n-alkane molecules. The solubility of water in different hydrocarbons is not identical because hydrocarbons, depending on their polarizability, engage in weak but variable van der Waals interactions with water (Wisniewska-Goclowska, Shaw, Skrzecz, Góral, & Maczynski, 2003).

Despite the technological importance of accurate data on mutual alkane-water solubilities, the available literature values are widely scattered and it is not easy to decide on a coherent set of data to use as reference.

The purpose of this work is the study and modeling of four binary water/alkane systems, water/n-hexane, water/n-heptane, water/n-undecane and water/n-hexadecane, using two different versions of the SAFT EoS. New unpublished solubility data of water in the n-alkanes obtained in our research group was used. SAFT-VR-SW, (Gil-Villegas, et al., 1997) and SAFT-$\gamma$-Mie (Lafitte, et al., 2013) versions of the theory were used to describe the mutual solubility of these specific water/n-alkane systems, but the study mainly focused on the alkane rich phase. Comparing the results from both theories is in itself of great importance. The thermodynamic functions of solution and solvation of water in the alkane rich phase, $\Delta_{sol}H_m^0$, $\Delta_{sol}S_m^0$, $\Delta_{svt}H_m^0$ and $\Delta_{svt}S_m^0$, were calculated for each system. The main goal of the analysis is to allow a better understanding of the water/n-alkanes interactions on the oil rich phase and in particular the dependence with the n-alkanes chain length.

## 1.2 State of the art

The importance of equations of state in Chemical Engineering can hardly be overestimated. The development of accurate molecular equations of state for the thermodynamic properties of fluids of associating molecules, is an important goal as it provides a framework for the representation of the behavior of real fluids and their mixtures with minimal computational cost. In the case of mixtures of water and alkanes, the microscopic nature of the associating interactions among water molecules is responsible for the extremely non-ideal conditions of the aqueous solutions of hydrocarbons, resulting in some anomalous properties that are challenging to model. Thus, the need to develop a thermodynamic modelling framework that considers anisotropic interactions (such as occur in hydrogen bonding fluids), molecular anisotropy (chain-like models and molecules), and electrostatics interactions (Coulombic, dipolar, quadrupolar) becomes increasingly acute, (Galindo & McCabe, 2010). It is also important to acknowledge the differences encountered in each phase, and therefore have a theory that can equally reproduce both phases.

One of the major advances in the theoretical modelling of complex fluids comes from the work of Wertheim (Wertheim, 1984) back in the 1980's, on associating and polymeric fluids and its implementation as an equation of state (EoS) by Champman, Gubbins, Radosz, and Jackson as the statistical associating fluid theory (SAFT), (Chapman, Gubbins, Jackson, & Radosz, 1989). Numerous versions of the SAFT EoS can be found today of which soft-SAFT (Blas & Vega, 1997), SAFT-VR (Gil-Villegas, et al., 1997), PC-SAFT (Gross & Sadowski, 2001) and SAFT-$\gamma$ –Mie (Lafitte, et al., 2013) are, perhaps, the main examples. SAFT-based equations became a powerful tool to predict thermodynamic properties and phase equilibria, due to its firm statistical mechanics basis and physical meaning of the description.

The statistical associating fluid theory, (Chapman, Gubbins,, Jackson, & Radosz, 1989), is a widely used molecular-based equation of state that has been successfully applied to study a broad range of fluid systems. It provides a framework in which the effects of molecular shape and interactions on the thermodynamics and phase behavior of fluids can be separated and quantified. In the SAFT approach molecules are modelled as associating chains formed of bonded spherical segments, with short ranged attractive sites, used as appropriate to mediate association interactions. The Helmholtz energy is written as the sum of four separate contributions:

$$\frac{\mathrm{A}}{\mathrm{Nk_B T}} = \frac{\mathrm{A_{Ideal}}}{\mathrm{Nk_B T}} + \frac{\mathrm{A_{Mono}}}{\mathrm{Nk_B T}} + \frac{\mathrm{A_{Chain}}}{\mathrm{Nk_B T}} + \frac{\mathrm{A_{Assoc.}}}{\mathrm{Nk_B T}} \qquad (1)$$

Where $A_{Ideal}$ is the ideal free energy, $A_{Mono.}$ the contribution to the free energy due to the monomer-monomer repulsion and dispersion interactions, $A_{Chain}$ the contribution due to the formation of bonds between monomeric segments, and $A_{Assoc.}$ the contribution due to association.

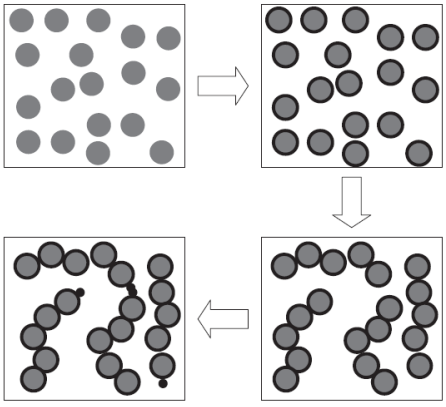

*Figure 1-Illustration of the perturbation scheme for a fluid within the SAFT framework. The reference fluid consists of spherical hard segments to which dispersion forces are added and chains can be formed through covalent bonds. Finally association sites allow for hydrogen bonding like interactions (Galindo & McCabe, 2010).*

In the original SAFT EoS for chains of Lennard-Jones segments, demonstrated in the work of (Chapman, Gubbins, Jackson, & Radosz, 1989), a perturbation expansion is used to describe the

monomer contribution and the hard-sphere radial distribution function is used to chain contribution. The simplest version of the theory involves associating chains of hard-sphere segments where the attractive interactions are treated at the mean-field van der Waals level, as described in the work of Chapman et al. This augmented van der Waals EoS for chain molecules is referred as the SAFT-HS approach, which gives a good description of the phase equilibria of several systems such as the critical behavior of n-alkanes, the high pressure critical lines of mixtures of alkanes and water and mixtures containing hydrogen fluoride.

There are numerous studies in the literature focusing on the application of different versions of the SAFT EoS to describe the water/alkane systems. Economou and Tsonopoulos used the associated-perturbed-anisotropic-chain-theory (APACT) and the statistical-associating-fluid-theory (SAFT) to predict the phase equilibrium of water/hydrocarbon mixtures, with emphasis on liquid/liquid equilibria (LLE), (Economou & Tsonopoulos, 1997). A more realistic mixing rule for these systems is proposed based on the asymmetric mixing rule introduced originally for the perturbed-hard-chain-theory (PHCT). This mixing rule is used for SAFT predictions of water/hydrocarbon LLE, resulting in an improvement of the hydrocarbon solubility predictions.

(Patel, Galindo, Maitland, & Paricaud, 2003) studied the salting out of *n*-alkanes in water by strong electrolytes using an extension of the statistical associating fluid theory for attractive potentials of variable range which incorporates ionic interactions. The systems are treated as water (1) + *n*-alkane (2) + cation (3) + anion (4) four-component mixtures. Since the scope of the present work involves only water/n-alkane mixtures, only these results will be presented and analyzed. The water molecules were modeled as spherical with four associating sites to mediate hydrogen bonding, while the *n*-alkane molecules are modeled as chains of tangentially bonded spherical segments interacting via square-well potentials. The phase behavior of the binary water/ *n*-alkane mixtures is well described by the theoretical approach using two unlike adjustable parameters, $\gamma_{ij}$ and $k_{ij}$, which are transferable for different alkane molecules.

*Table 1- m, λ, σ (Å) and ε/k, $\epsilon^{HB}$/k (K) and K(Å)used for the water model of SAFT-VR (Patel, Galindo, Maitland, & Paricaud, 2003)*

| Compound | m | λ | σ (Å) | ϵ/k (K) | $\epsilon^{HB}$/k (K) | K ($Å^3$) |
|---|---|---|---|---|---|---|
| Water | 1 | 1,8 | 3,036 | 253,3 | 1366 | 1,028 |
| n- hexane | 2,6667 | 1,552 | 3,92 | 250,4 | 0 | 0 |

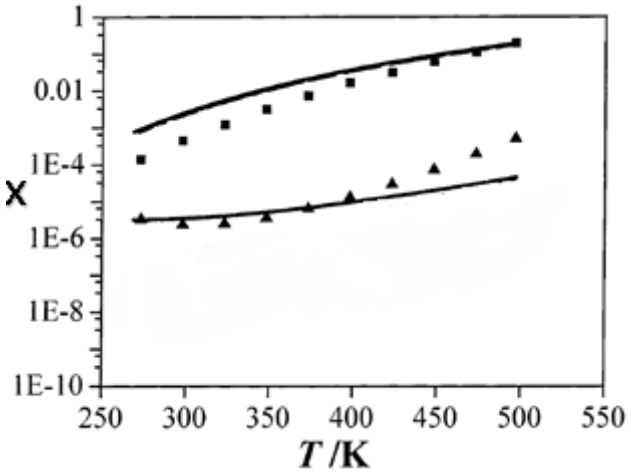


*Figure 2- The symbols correspond to the experimental data composition: n-hexane in the water rich phase (triangles) and the water in the alkane rich phase (squares). Solid curves correspond to the SAFT-VR calculations for a mixture of water/n-hexane (Patel, Galindo, Maitland, & Paricaud, 2003).*

Patel et al, found that it was possible to reproduce the minimum in solubility by using two adjustable parameters $k_{ij}$ and $\gamma_{ij}$, which determine the strength of the unlike dispersion interaction, for the water/n-hexane. The found values for the $k_{ij}$ and $\gamma_{ij}$ were, respectively -0,74165 and the $\gamma_{ij}$ 0,22043. It is important to note that the work of Patel, was more focused on the description of the water rich phase.

Vega, Lovel and Blas published a study where they were able to capture the solubility minima of *n*-alkanes in water using soft-SAFT. The purpose of their work was to find a molecular model for water, within the soft-SAFT framework, capable of describing the water/n-alkanes mixtures at room temperature. The model was used to describe the water/methane up to water / *n*-decane binary mixtures. The equation was able to predict the mutual solubilities, with a single transferable energy binary parameter, $\xi$, independent of temperature and chain length, (Vega, Llovell, & Blas, 2009). The soft-SAFT version of the SAFT theory (Johnson, Muller, & Gubbins, 1994) treats alkanes as chains of Lennard-Jones segments. The free energy of the chain fluid is obtained from the free energy and radial distribution function of the monomer Lennard-Jones fluid. These expressions were fitted to simulation data. Soft-SAFT is thus a very accurate equation for Lennard-Jones chains and for modelling mixtures of associating Lennard-Jones fluids, since is heavily based on simulation data. This approach has been applied to the study of alkanes and their binary and ternary mixtures, perfluoralkanes, alcohols, carbon dioxide polymers and ionic liquids. Soft-SAFT has been recently developed by Vega et al, to model mixtures of water and alkanes. In the work of (Vega, Llovell, & Blas, 2009) the molecular parameters of the n-alkanes were taken from published correlations with the molecular weight of the compounds, (Blas & Vega, 1998) and (Blas & Vega, 1998). Water was modeled as a Lennard-Jones sphere with four associating sites, with parameters obtained by fitting to experimental vapor-liquid equilibrium data.

*Table 2*-Molecular parameters for a four associating sites model for water using soft-SAFT *(Vega, Llovell, & Blas, 2009)*

| **Procedure** | **m** | $\boldsymbol{\sigma}$(Å) | $\epsilon/\boldsymbol{k_B}$**(K)** | $\boldsymbol{K^{HB}}$ **(Å$^3$)** | $\epsilon^{\boldsymbol{HB}}/\boldsymbol{k_B}$**(K)** |
|---|---|---|---|---|---|
| T range from 300-450K | 1 | 3,154 | 365 | 2932 | 2388 |

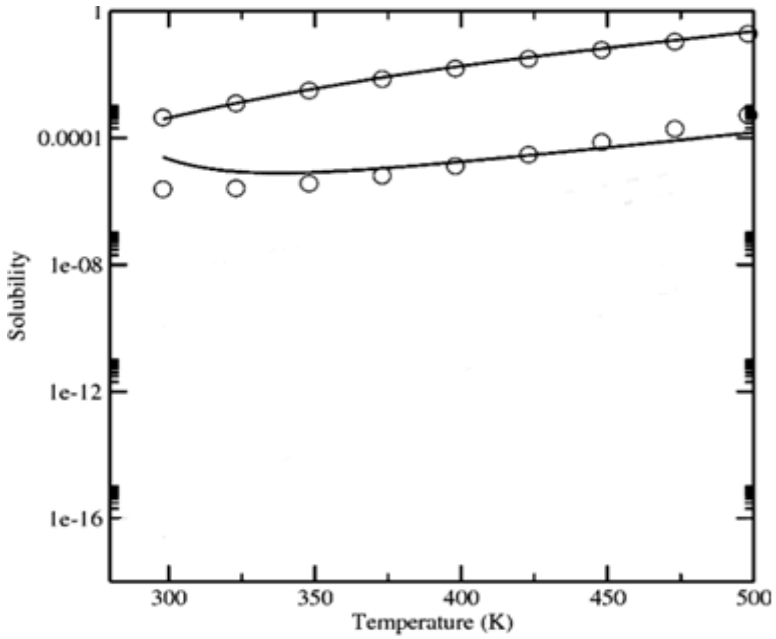


*Figure 3- Solid line represent results obtained with soft-SAFT EoS and black circles experimental data, (Vega, Llovell, & Blas, 2009)*

A binary interaction parameter, $k_{ij}$, was used to fit the mutual solubility of the water/n-hexane system. An optimal value of 0,32 was used for both phases. As can be seen in the figure the soft-SAFT results are in close agreement with the experimental data from (Tsonopoulos & Wilson, 1983) for the alkanes rich phase. For the water rich phase the agreement is not as good, but the theory is able to describe the solubility minimum of alkanes in water. For a deeper understanding the reader is directed to the original papers (Llóvell, Pàmies, & Vega, 2004).

In the last years, many developments have been accomplished, and the SAFT expressions are continually being improved. An accurate representation of the monomer-monomer distribution function has been included to deal with chains of Lennard-Jones segments and the approach has been extended to different types of monomer segments such as square wells and more recently Mie segments.

# Chapter 2

## SAFT-VR-SW

It was in the work of Gill-Villegas, Galindo, Whitehead, Mills and Jackson, that the SAFT-VR was first introduced, a general version of SAFT for chain molecules formed from hard-core monomers with an arbitrary potential of variable range, VR, (Gil-Villegas, et al., 1997). This approach was also extended to soft-core potentials and mixtures. Compared with the SAFT-HS approach, SAFT-VR is a step further improving the chain contribution and the mean-field Van der Waals description for the dispersion forces of the SAFT-HS treatment. The SAFT-VR approach also provides additional parameters that characterize the range of the attractive part of the monomer-monomer potential. Throughout chapter 2, the version of SAFT-VR used in this work will be presented along with the obtained results.

The SAFT-VR equation has been extensively tested against simulation data and successfully used to describe the phase equilibria of a wide range of industrially important systems, such as alkanes of low molar mass, simple polymers and their binary mixtures, perfluoroalkanes, alcohols, water refrigerant systems and carbon dioxide have all been studied. (Galindo & McCabe, 2010)

In the present work the SAFT-VR-SW was used to obtain solubility data of different water/n-alkanes systems. In this section a brief description of the theory is presented. For further insight on the SAFT- VR-SW approach the reader is referred to the original SAFT-VR-SW paper where a more detailed description of the expressions can be found, (Gil-Villegas, et al., 1997) and (McCabe C. , Galindo, GiI-Villegas, & Jackson, 1998).

## The intermolecular potential model

SAFT was extended to describe associating chain molecules formed from hardcore monomers with attractive potentials of variable range in the SAFT-VR equation. Although, in the original publication, several potentials of variable range were studied, square-well, LJ, Mie and Yukawa, typically a square-well potential is implemented in the modelling of real fluids.

The considered hard-core potential used in this work is the square-well in which both repulsive and attractive interactions are included. It can be defined as,

$$u^{SW}(r) = \begin{cases} \infty \; if \; r < \sigma \\ -\epsilon \; \text{if} \; \sigma \leq r \leq \lambda\sigma \\ 0 \; \text{if} \; r > \lambda\sigma \end{cases} \tag{2}$$

where *r* is the intermolecular centre-to-centre distance, $\sigma$ the hardcore diameter, $\epsilon$ the depth of the attractive well and $\lambda$ its range. In the square well, the energy is constant over the range of interaction.

To better illustrate the square well potential segment-segment interaction, figure 2 is represented.

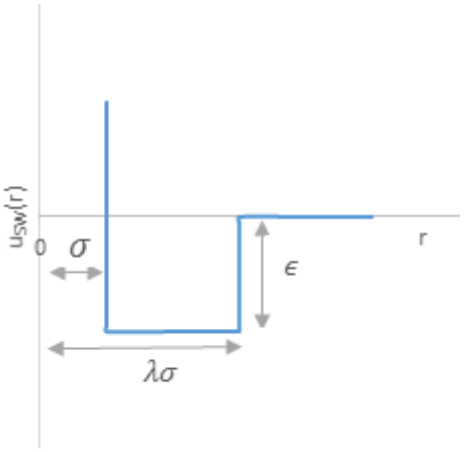


*Figure 4- Square well potential segment-segment interaction*

In order to obtain the Helmholtz free energy is necessary to calculate the four different terms, given by the following expressions.

## Ideal term

The free energy of an ideal gas is given as by,

$$\frac{\mathrm{A^{ideal}}}{\mathrm{Nk_BT}} = (\sum_{i=1}^{n} x_i \ln(\rho_i \Lambda_i^3))\text{-}1 \qquad (3)$$

Where $x_i = {}^{N_i}/_{N}$ is the mole fraction, $\rho_i = {}^{N_i}/_{V}$ is the molecular number density, $N_i$ is the number of molecules, $\Lambda_i$ is the thermal de Broglie wavelength of species *i,* and *V* is the volume of the system Since the ideal term is treated separately, the other terms are all excess free energies.

## Monomer term

The monomers contribution to the Helmholtz free energy (m of which make up each chain) is given by the following expression,

$$\frac{\mathrm{A^{mono.}}}{\mathrm{Nk_BT}} = \left(\sum_{i=1} x_i m_i\right) \frac{\mathrm{A^M}}{\mathrm{N_s k_B T}} = \left(\sum_{i=1} x_i m_i\right) \mathrm{a^M} \qquad (4)$$

For which $m_i$ is the number of spherical segments of chain *i*, $N_s$ is the total number of spherical monomers, and $a^M$is the excess Helmholtz free energy per monomer.

## Chain term

The contribution to the free energy due to the formation of a chain of *m* monomers is,

$$\frac{\mathrm{A^{chain}}}{\mathrm{Nk_B T}} = -\left(\sum_{i=1}^{n} x_i(m_i - 1)\right) \ln y_{ii}^{SW}(\sigma_{ii}) \tag{5}$$

## Association Term

The contribution due to association for *s* sites on chain molecules is obtained from,

$$\frac{\mathrm{A^{Assoc.}}}{\mathrm{Nk_B T}} = \left[\sum_{\mathrm{a}=1}^{\mathrm{s}} \left(\ln \mathrm{X_a} - \frac{\mathrm{X_a}}{2}\right) + \frac{\mathrm{s}}{2}\right] \tag{6}$$

taking in account that the sum is over all *s* sites *a* on a molecule, and that $X_a$ is the fraction of molecules not bonded at site *a,* $X_a$ is then obtained by a solution of the following mass action equation.

## Water Model

The water molecule with its two hydrogen atoms bonded to an oxygen atom, may seem like a simple molecule, but its polarity and the steric features of its geometry give rise to complicated intermolecular forces. The structure of the water molecule is due to the short-range forces with the clustering being given by the formation of directional hydrogen bonds. Numerous studies of the fluid phase equilibria of pure water and aqueous mixtures, (Clark G. , Haslam, Galindo, & Jackson, 2006), have been made within the various incarnations of the SAFT theory, but there still is no consensus on or what the association scheme should be (two-, three-, or four-site models). In this work the chosen model is the four-site water model illustrated in the following figure.

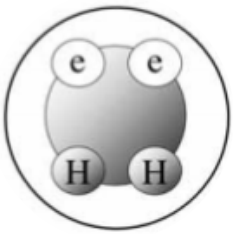


*Figure 5-Ilustration of the four site (2H and 2e) model of water, (Clark G. N., Haslam, Galindo, & Jackson, 2006)*

In this model the two hydrogen bonding interactions are mediated through off-center square-well bonding sites of types *H* (Hydrogen) and *e* (electron lone pairs), located halfway between the center and the surface of the molecular core. Only *e-H* bonding is considered, and multiple bonding at a given site is forbidden. When an *e* and an *H* site come within a cut-off range $r_{c;H,e}$ of each other there is a site-site hydrogen-bonding associative interaction. The parameters used for the four-site water model are displayed in table 3.

## Combining rules

The study of phase equilibria in mixtures requires the determination of a number of unlike parameters. In the SAFT-VR approach the used combining rules are presented in the following expressions, (McCabe C. , Galindo, Gil-Villegas, & Jackson, 1998).

The unlike size is calculated using the Lorentz rule,

$$\sigma_{ij} = \frac{\sigma_{ii} + \sigma_{jj}}{2} \tag{7}$$

Where the energy parameters are calculated recurring to the following equation,

$$\epsilon_{ij} = (1 - k_{ij})\sqrt{\epsilon_{ii}\epsilon_{jj}} \tag{8}$$

In the above equation, the adjustable coefficient, describes the departure of the system from the Berthelot rule. It is also important to note that the adjustable parameter $k_{ij}$can also be presented in the following expression,

$$\xi = 1 - k_{ij} \tag{9}$$

The unlike range parameter is obtained from the arithmetic mean of the pure component values, through the following equation, it is important to note that in the present work the value of the adjustable parameter, $\gamma_{ij}$, was considered 0.

$$\lambda_{ij} = (1 - \gamma_{ij})\frac{\lambda_{ii}\sigma_{ii} + \lambda_{jj}\sigma_{jj}}{\sigma_{ii} + \sigma_{jj}} \tag{10}$$

## Results

In the light of the previous treatments presented, the results obtained in this work using SAFT-VR-SW are now presented. The scope of the present work resides in finding an adjustable parameter, $k_{ij}$ capable of describing the oil rich phase of the four binary water/n-alkane systems, obtained within our research group. Throughout the following figures, the solubility of water and its dependence with temperature for both experimental data and the SAFT-VR-SW prediction is presented.

In order to study the influence of the binary interaction parameter, $k_{ij}$, on the description of the water/n-alkane systems two predictions were made: one in which the value of $k_{ij}$, was considered zero and another on which the value of $k_{ij}$ was adjusted to the oil rich phase experimental data of (Morgado, 2011). In the following figures the experimental data is from (Morgado, 2011) and (Maczynski A. , Shaw, Goral, & Wisniewska-Goclowska, 2005).

The parameters characterizing the chosen water model were optimized to vapour–liquid equilibria data from the triple point to 90% of the critical temperature, (Clark G. N., Haslam, Galindo, &

Jackson, 2006). The parameters λ, σ and ε/k used to describe each compound with SAFT-VR-SW were those reported by (Paricaud, Jackson, & Galindo, 2004) obtained optimizing the description of the experimental vapor pressure and density for the various alkanes.

*Table 3- m, λ, σ (Å) and ϵ /k used for the water model of SAFT-VR-SW (Clark G. N., Haslam, Galindo, & Jackson, 2006)*

| Compound | λ | σ (Å) | ϵ /k (K) | $\epsilon^{HB}$ /k (K) | $r_c^{HB}$(Å) | $K^{HB}$(Å³) |
|---|---|---|---|---|---|---|
| **Water** | 1,7889 | 3,0342 | 250 | 1400,00 | 2,1082 | 1,0667 |

*Table 4- m, λ, σ (Å) and ε/k used for each studied compound using SAFT-VR-SW taken from (Paricaud, Jackson, & Galindo, 2004)*

| Compound | m | λ | σ (Å) | ϵ/k (K) |
|---|---|---|---|---|
| n-hexane | 2,6667 | 1,5492 | 3,9396 | 251,66 |
| n-heptane | 3,0000 | 1,5574 | 3,9567 | 253,28 |
| n-undecane | 4,3333 | 1,5854 | 3,9775 | 252,65 |
| n-hexadecane | 6,0000 | 1,6325 | 3,9810 | 237,33 |

The theoretical predictions for all systems are compared with the experimental data in figures 6-9.

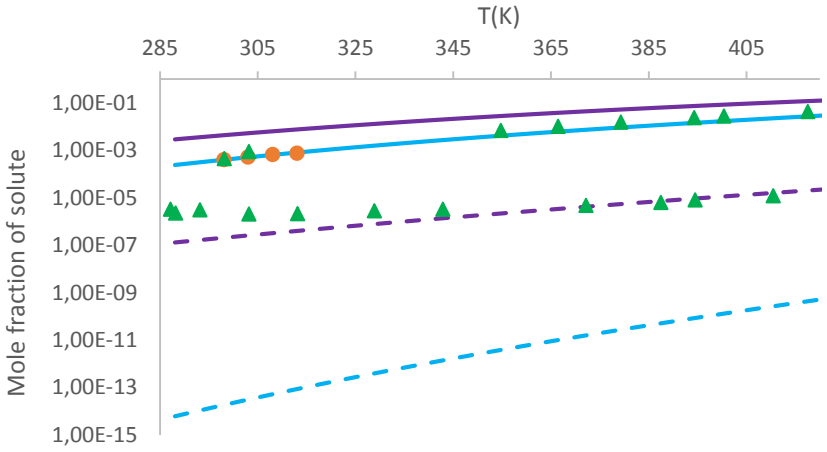


*Figure 6- Mole fraction of water in n-hexane (solid line) and of n-hexane in water (dotted line) as a function of temperature; triangles represent experimental data from (Maczynski A. , Shaw, Goral, & Wisniewska-Goclowska, 2005); filled circles represent experimental data from (Morgado, 2011); purple line represents prediction from SAFT-VR-SW (tab 4) with $k_{ij}$=0 and the blue line with the $k_{ij}$=0,30.*

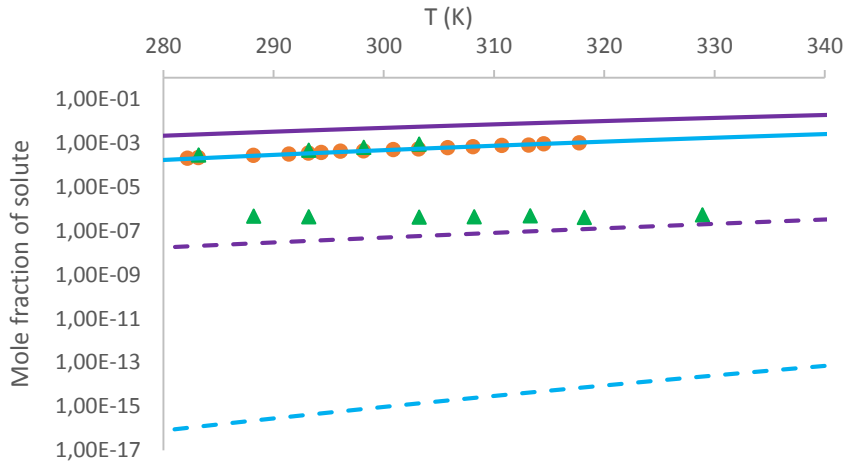


*Figure 7- Mole fraction of water in n-heptane (solid line) and of n-heptane in water (dotted line) as a function of temperature; triangles represent experimental data from (Maczynski A. , Shaw, Goral, & Wisniewska-Goclowska, 2005); filled circles represent experimental data from (Morgado, 2011); purple line represents prediction from SAFT-VR-SW (tab 4) with kij=0 and the blue line with the $k_{ij}$=0,29.*

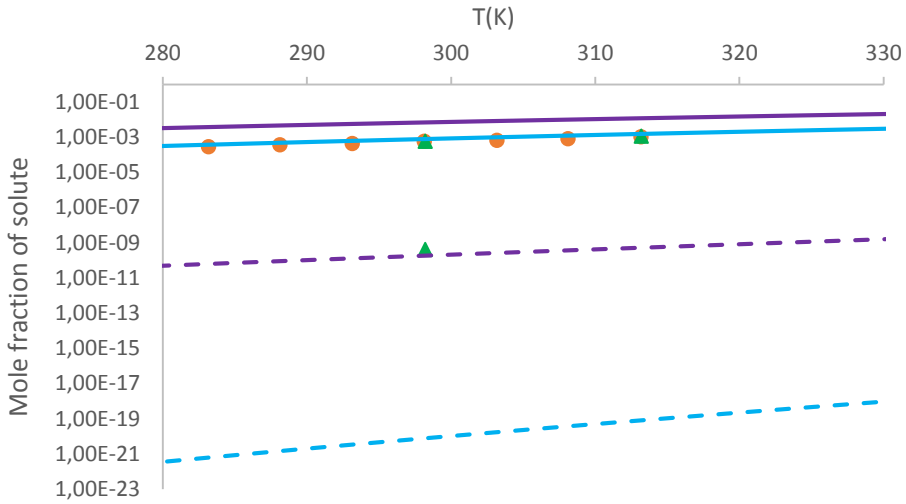


*Figure 8- Mole fraction of water in n-undecane (solid line) and of n-undecane in water (dotted line) as a function of temperature; triangles represent experimental data from (Maczynski A. , Shaw, Goral, & Wisniewska-Goclowska, 2005); filled circles represent experimental data from (Morgado, 2011); purple line represents prediction from SAFT-VR-SW (tab 4) with $k_{ij}$=0 and the blue line with the $k_{ij}$=0,26.*

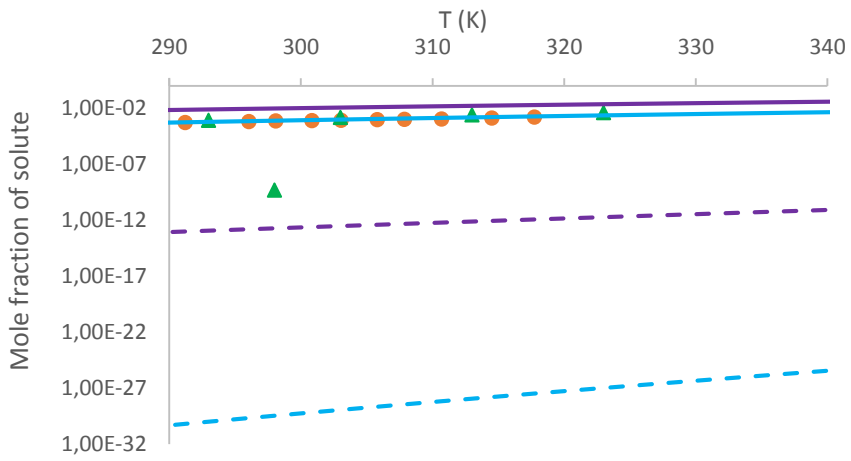


*Figure 9- Mole fraction of water in n-hexadecane (solid line) and of hexadecane in water (dotted line) as a function of temperature; triangles represent experimental data from (Maczynski A. , Shaw, Goral, & Wisniewska-Goclowska, 2005); filled circles represent experimental data from (Morgado, 2011); purple line represents prediction from SAFT-VR-SW (tab 4) with kij=0 and the blue line with the $k_{ij}$=0,30.*

As can be observed, in all systems the theoretical predictions with $k_{ij}$=0 overpredict the experimental solubility of water in the hydrocarbon-rich phase (solid line). For the water-rich phase (square dot line), in the case of water/n-heptane, n-undecane and n-hexadecane, the theoretical results underpredict the experimental solubility, although in the case of water/n-undecane the prediction is very close to the experimental value. In the case of water/n-hexane, however, the theoretical results are in good agreement with the experimental results at the higher temperatures (higher than 340K), but underpredict at lower temperatures. It is also important to note that the shape of the curve in the water rich phase does not follow the trend of the experimental results.

Analyzing the results for which the $k_{ij}$ was fitted to the (Morgado, 2011) experimental data, one can see that for all systems the prediction for the oil rich phase is very good, better than in the previous case ($k_{ij}$=0). However, the predicted solubility of the n-alkanes in the water rich phase is largely underpredicted. These results demonstrate that optimizing the $k_{ij}$ values to reproduce the experimental solubility of water in the n-alkanes lowers both sides of the system's curves resulting in a very good prediction on the oil rich phase but in much worse results on the water rich phase.

The following figure summarizes the obtained results. As it can be observed, if only the water/n-hexane, water/n-heptane and water/n-undecane are considered, the optimal $k_{ij}$ value decreases with the chain length, but that is not observed for the water/n-hexadecane for which the optimal $k_{ij}$ value is 0,30, the same as the $k_{ij}$ found for the n-hexane.

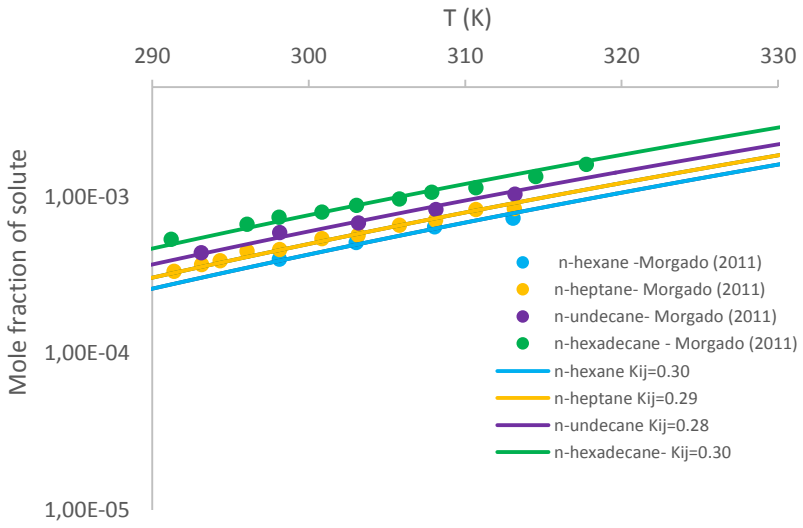


*Figure 10- Solubility of water in n-alkanes, experimental data (Morgado, 2011) (circles) and predicted by SAFT-VR-SW (tab 2) for different temperatures.*

# Chapter 3

## SAFT-γ-Mie Group Contribution approach

The latest development of the statistical associating fluid theory family is a generalization for variable range Mie potentials (Lafitte, et al., 2013) and is formulated within the framework of a group contribution approach, SAFT-γ-Mie. Molecules are represented as comprising distinct functional chemical groups based on a fused heteronuclear molecular model, where the interactions between segments are described with the Mie potential of variable attractive and repulsive range. The group-contribution (GC) approach represents an alternative to the homonuclear approach present in other SAFT versions, the GC model has also been applied not just to the SAFT- γ approach but also to SAFT-VR.

An advantage of this model is the ability to obtain predictions of thermodynamic properties of pure components and mixtures based on segment data. The GC concept has been employed within a SAFT formalism based on a more detailed heteronuclear molecular model, with different types of monomeric segments used to describe the different chemical/functional groups constituting a given molecule.

A particular advantage of the Mie potential is the ability to modify the detailed form of the pair interaction potential between segments, adjusting the values of the repulsive and attractive exponents. Hence, it is possible to capture the finer features of the interaction, which are important to provide an accurate description of the thermodynamic derivative properties.

In this work besides the SAFT-VR-SW theory also the SAFT-γ-Mie Group contribution approach was used to obtain results on the studied water/n-alkane systems. In this section, the main aspects of the SAFT-γ-Mie Group contribution are presented, being the reader referred to the original papers for deeper insight (Papaioannou, et al., 2014).

## Molecular model and intermolecular potential

As it was mentioned before, the most recent version of SAFT-based group-contribution approaches is the SAFT-γ Mie EoS, where a heteronuclear model is implemented and the segment-segment interactions are represented by Mie potential of variable repulsive and attractive range.

In order to better illustrate the molecular model implemented to describe the molecules within this approach, the next figure is a representation of the n-hexane molecule.

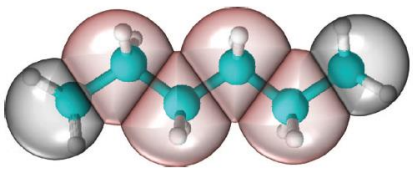

*Figure 11- Representation of n-hexane within the SAFT- $\gamma$ Mie approach, where the molecule is described as fused heteronuclear segments. This molecular model comprises two instances of the methyl CH3 group (highlighted in gray), and four instances of the methylene CH2 group (highlighted in red), (Papaioannou, et al., 2014)*

Each chemical functional group *k* (e.g. CH3, CH2) is represented as a fused spherical segment or number of segments $v_k^*$. Two segments *k* and *l* are assumed to interact via a Mie potential of variable range:

$$\Phi_{\mathrm{kl}}^{\mathrm{Mie}}(\mathrm{r_{kl}}) = \mathrm{C_{kl}}\epsilon_{\mathrm{kl}}\left[\left(\frac{\sigma_{\mathrm{kl}}}{\mathrm{r_{kl}}}\right)^{\lambda_{\mathrm{kl}}^{\mathrm{r}}} - \left(\frac{\sigma_{\mathrm{kl}}}{\mathrm{r_{kl}}}\right)^{\lambda_{\mathrm{kl}}^{\mathrm{a}}}\right] \tag{11}$$

where $\mathrm{r_{kl}}$ is the distance between the centres of the segments, $\sigma_{\mathrm{kl}}$ the segment diameter, $\epsilon_{\mathrm{kl}}$ the depth of the potential well, and $\lambda_{kl}^{r}$ and $\lambda_{kl}^{a}$ the repulsive and attractive exponents of the segment-segment interactions, respectively. The prefactor $\mathrm{C_{kl}}$ is a function of these exponents and ensures that the minimum of the interaction is -$\epsilon_{\mathrm{kl}}$.

$$\mathrm{C_{kl}} = \frac{\lambda_{\mathrm{kl}}^{\mathrm{r}}}{\lambda_{\mathrm{kl}}^{\mathrm{r}} - \lambda_{\mathrm{kl}}^{\mathrm{a}}}\left(\frac{\lambda_{\mathrm{kl}}^{\mathrm{r}}}{\lambda_{\mathrm{kl}}^{\mathrm{a}}}\right)^{\frac{\lambda_{\mathrm{kl}}^{\mathrm{a}}}{\lambda_{\mathrm{kl}}^{\mathrm{r}} - \lambda_{\mathrm{kl}}^{\mathrm{a}}}} \tag{12}$$

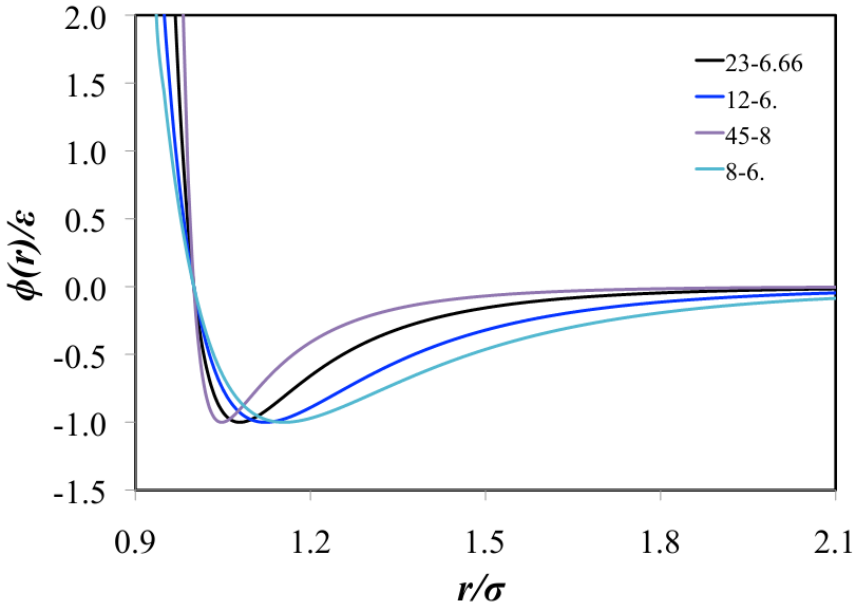


*Figure 12- Different Mie potential representations from hard to soft potentials, (12-6) Lennard-Jones potential, (45-8) hard potential, (8-6) soft potential and (23- 6,6), (Rodrigues, 2012).*

The Helmholtz free energy of this model can be obtained from the appropriate contributions of the different groups, noting that the implementation of this type of united-atom model of fused segments requires the additional use of a shape factor $S_k$, which reflects the proportion in which a given segment contributes to the total free energy. As in other SAFT approaches, hydrogen bonding or strongly polar interactions can be treated through the incorporation of a number of additional short-range square-well association sites, which are placed on any given segments as required. The association interaction between two square-well association sites of type *a* in segment *k* and *b* in segment *l* is given by,

$$\Phi^{\mathrm{HB}}_{\mathrm{kl,ab}}\left(\mathrm{r}_{\mathrm{kl,ab}}\right) = \begin{cases} -\epsilon^{\mathrm{HB}}_{\mathrm{kl,ab}} \text{ if } \mathrm{r}_{\mathrm{kl,ab}} \leq \mathrm{r}^{\mathrm{c}}_{\mathrm{kl,ab}}\,, \\ 0 \text{ if } \mathrm{r}_{\mathrm{kl,ab}} > \mathrm{r}^{\mathrm{c}}_{\mathrm{kl,ab}}\,, \end{cases} \tag{13}$$

where $r_{kl,ab}$ is the center-center distance between sites *a* and *b*, $-\epsilon^{HB}_{kl,ab}$ is the association energy, and $r^{c}_{kl,ab}$ the cut-off range of the interaction between sites *a* and *b* on groups *k* and *l*, respectively. Each site is positioned at a distance $r^{d}_{kk,aa}$ from the center of the segment on which it is placed.

In summary, a functional group k is fully described by the number $v^{*}_{k}$ of identical spherical segments forming the group, the shape factor of the segments $S_k$, the diameter of the segments $\sigma_{kk}$ of the group, the segment energy of interaction $\epsilon_{kk}$ of the group, and the repulsive and attractive exponents of the Mie potential $\lambda^{r}_{kk}$ and $\lambda^{a}_{kk}$, respectively, as well as the parameters characterizing any site-site association interactions. The interactions between groups of different types *k* and *l* are specified through the corresponding unlike parameters $\sigma_{kl}$, $\epsilon_{kl}$, $\lambda^{r}_{kl}$, $\lambda^{a}_{kl}$. In the case of

associating groups, the number $N_{ST,k}$ of different site types, the number of sites of a given type, e.g., $n_{k,a}$, $n_{k,b}$,…, $n_{k,N_{ST,k}}$, together with the position $r^{d}_{kl,ab}$of the site, and the energy $\epsilon^{HB}_{kl,ab}$ and range of $r^{c}_{kl,ab}$ of the association between sites, of the same or different type, have to be determined.

## The ideal term

The free energy corresponding to an ideal mixture of molecules is given by the following expression,

$$\frac{\mathrm{A^{ideal}}}{\mathrm{Nk_B T}} = \left( \sum_{\mathrm{i=1}}^{\mathrm{N_C}} \mathrm{x_i ln}(\rho_\mathrm{i} \Lambda_\mathrm{i}^3) - 1 \right) \tag{14}$$

where $x_i$ is the mole fraction of component *i* in the fraction, $\rho_i$ = $\frac{N_i}{V}$ the number density of component *i*, being $N_i$ the number of molecules of component *i* and *V* the total volume of the system, *N* the total number of molecules, $k_B$ the Boltzmann constant, and *T* the absolute temperature. The summation is over all of the components $N_C$ of the mixture. The ideal free energy incorporates the effects of the translational, rotational and vibrational contributions to the kinetic energy implicitly in the thermal de Broglie volume $\Lambda_i^3$.

## The monomer term

The free-energy contribution due to repulsion and attraction interactions for the monomeric fluid characterized by the Mie potential is obtained following a Barker-Henderson high temperature perturbation expansion up to third order, which can be expressed as

$$\frac{\mathrm{A^{mono.}}}{\mathrm{Nk_B T}} = \frac{\mathrm{A^{HS}}}{\mathrm{Nk_B T}} + \frac{\mathrm{A_1}}{\mathrm{Nk_B T}} + \frac{\mathrm{A_2}}{\mathrm{Nk_B T}} + \frac{\mathrm{A_3}}{\mathrm{Nk_B T}} \tag{15}$$

where the repulsive term $A^{HS}$ is the free energy of a hard-sphere reference system of diameter $d_{kk}$, dependent of the temperature. In the SAFT-$\gamma$ group-contribution approach each of the segment's contribution to the free energy is added with the next expression,

$$\frac{\mathrm{A^{HS}}}{\mathrm{Nk_B T}} = \left( \sum_{\mathrm{i=1}}^{\mathrm{N_C}} \mathrm{x_i} \sum_{\mathrm{k=1}}^{\mathrm{N_G}} \mathrm{v_{k,i} v_k^* S_k} \right) \mathrm{a^{HS}} \tag{16}$$

With $N_G$ as the number of types of groups present, $v_{k,i}$ the number of occurrences of a group of type *k* on component *i*, and $a^{HS}$ is the dimensionless contribution to the hard-sphere free energy per segment, obtained using the expression of (Boublík, 1971) and (Mansoori, Carnahan, Starling, & Leland, 1971) .

The subsequent terms in the expansion are obtained following similar summations over the free-energy contributions per segment, each with their corresponding power of inverse temperature, so that the mean attractive energy, the energy fluctuation, and the third-order terms are given by,

$$\frac{A_q}{Nk_BT} = \left(\frac{1}{k_BT}\right)^q \left(\sum_{i=1}^{N_C} x_i \sum_{k=1}^{N_G} v_{k,i} v_k^* S_k\right) a_q, q = 1,2,3 \quad (17)$$

The free energy contributions per segment $a_q$ are obtained, as for the hard-sphere reference term, by summing the pairwise interactions $a_{q,kl}$ between groups *k* and *l* over all pairs of functional groups present in the system,

$$a_q = \sum_{k=1}^{N_G} \sum_{l=1}^{N_C} x_{s,k}\, x_{s,l} a_{q,kl}, \qquad q = 1,2,3 \quad (18)$$

explicit expressions for these can be found in the work of (Lafitte, et al., 2013)

## Chain term

In the SAFT-*γ* approach the change in free energy associated with the formation of a molecule from its constituting segments is obtained recurring to the average molecular parameters ($\overline{\sigma_{ii}}$, $\overline{d_{ii}}$, $\overline{\epsilon_{ii}}$ and $\overline{\lambda_{ii}}$), for each molecular species *i*. The resulting contribution to the free energy of the mixture due to the formation of chains of tangent (or fused) segments using the effective molecular parameters is given by

$$\frac{A^{chain}}{Nk_BT} = -\sum_{i=1}^{N_C} x_i \left(\sum_{k=1}^{N_G} v_{k,i} v_k^* S_k - 1\right) \ln g_{ii}^{Mie}(\overline{\sigma_{ii}}; \zeta_x) \quad (19)$$

where $g_{ii}^{Mie}(\overline{\sigma_{ii}}, \zeta_x)$ is the value of the radial distribution function (RDF) evaluated at a distance $\overline{\sigma_{ii}}$ in a hypothetical fluid of packing fraction $\zeta_x$, defined as $\zeta_x = \frac{\pi}{6}\rho_s \sum_{k=1}^{N_G} \sum_{l=1}^{N_C} x_{s,k}\, x_{s,l} a_{q,kl}$.

## Association Term

Deriving from the original TPT1 expressions of Wertheim, the contribution to the Helmholtz free energy due to the association of molecules via short range bonding sites is obtained by summing over the number of species $N_C$, the number of groups $N_G$, and the number of site types on each group $N_{ST,k}$, as showed in the following equation,

$$\frac{A^{assoc.}}{Nk_BT} = \sum_{i=1}^{N_C} x_i \sum_{k=1}^{N_G} v_{k,i} \sum_{a=1}^{N_{ST,k}} n_{k,a} \left(\ln X_{i,k,a} + \frac{1 - X_{i,k,a}}{2}\right) \quad (20)$$

Where $n_{k,a}$is the number of sites of type *a* on group *k*, and $X_{i,k,a}$is the fraction of molecules of component *i*, that are not bonded at a site of type *a* on a group *k*.

## Water Model

Group contribution techniques are generally not well suited for the study of small molecules as proximity effects are neglected, to have a more accurate model the water molecule is described

as a separate functional group, capable only of associating between sites *H* and *e*. This water model is described by the parameters in tables 5,6 and 7.

## Combining Rules

The study of binary and multicomponent systems requires a number of combining rules for the unlike intermolecular parameters. These are typically determined using combining rules, and refined by estimation from experimental data when required. However, as a consequence of the use of a heteronuclear model in the SAFT-*γ* EOS, the unlike group interactions are required not only to treat mixtures, but also for pure component calculations.

The unlike segment diameter is obtained from a simple arithmetic mean,

$$\sigma_{\mathrm{kl}} = \frac{\sigma_{\mathrm{kk}+}\sigma_{\mathrm{ll}}}{2} \tag{21}$$

For the calculation of the unlike effective hard-sphere diameter, the same combining rule is applied,

$$\mathrm{d}_{\mathrm{kl}} = \frac{\mathrm{d}_{\mathrm{kk}+}\mathrm{d}_{\mathrm{ll}}}{2} \tag{22}$$

As for the unlike dispersion energy, $\epsilon_{kl}$, the system's mixture data is used since no pure molecule contains the interaction water -CH2 or water –CH3.

The combining rule for the repulsive, ${\lambda_{kl}}^{r}$, and the attractive, ${\lambda_{kl}}^{a}$ is given by equation 23.

$$\lambda_{\mathrm{kl}} = 3 + \sqrt{(\lambda_{\mathrm{kk}} - 3)(\lambda_{\mathrm{ll}} - 3)} \tag{23}$$

The unlike value of the association energy can be obtained by means of a simple geometric mean rule,

$${\epsilon_{\mathrm{kl}}}^{\mathrm{HB}} = \sqrt{{\epsilon_{\mathrm{kk,aa}}}^{\mathrm{HB}}{\epsilon_{\mathrm{ll,bb}}}^{\mathrm{HB}}} \tag{24}$$

The unlike bonding volume $K_{\mathrm{kl,ab}}$ is obtained with equation 25.

$$K_{\mathrm{kl,ab}} = \left(\frac{\sqrt[3]{K_{\mathrm{kk,aa}}} + \sqrt[3]{K_{\mathrm{ll,bb}}}}{2}\right)^{3} \tag{25}$$

Also, a number of combining rules for the average molecular parameters required for the calculation of the chain and association contributions to the free energy also need to be considered. The unlike values for the effective segment size, $\bar{\sigma}_{ij}$ and $\bar{d}_{ij}$, dispersion energy,$\bar{\epsilon}_{ij}$ , and repulsive and attractive exponents of the potential, $\bar{\lambda}_{ij}$, are obtained from the following expressions,

$$\bar{\sigma}_{ij} = \frac{\bar{\sigma}_{ii} + \bar{\sigma}_{jj}}{2} \tag{26}$$

$$\bar{d}_{ij} = \frac{\bar{d}_{ii} + \bar{d}_{jj}}{2} \tag{27}$$

$$\bar{\epsilon}_{ij} = \frac{\sqrt{\bar{\epsilon}_{ii}^{3}\bar{\epsilon}_{jj}^{3}}}{\bar{\epsilon}_{ij}^{3}}\left(\sqrt{\bar{\epsilon}_{ii}\bar{\epsilon}_{jj}}\right) \tag{28}$$

$$\bar{\lambda}_{ij} = 3 + \sqrt{(\bar{\lambda}_{ii} - 3)(\bar{\lambda}_{jj} - 3)} \tag{29}$$

The parameters used to describe each system with SAFT- γ-Mie, taken from (Dufal, Papaioannou, Sadeqzadeh, & Pogiatzis, 2014) are displayed in tables 6 and 7.

*Table 5- Group parameters within the SAFT-γ Mie group-contribution approach used in the present work: $v_k^*$,the number of segment constituting group k , $S_k$, the shape factor, $\lambda^r_{kk,}$ the repulsive exponent, $\lambda^a_{kk,}$ the attractive exponent, $\sigma_{kk}$ [Å], the segment diameter of group k, ($\epsilon_{kk}/k_B$) the dispersion energy of the Mie potential characterizing the interaction of two k groups; (K). (Dufal, Papaioannou, Sadeqzadeh, & Pogiatzis, 2014).*

| Group | $vk^*$ | $S_k$ | $\lambda^r_{kk}$ | $\lambda^a_{kk}$ | $\sigma_{kk}$ [Å] | ($\epsilon_{kk}/k_B$) (K) |
|---|---|---|---|---|---|---|
| H2O | 1 | 1,0000 | 17,0504 | 6 | 3,01 | 266,684 |
| CH3 | 1 | 0,5726 | 15,0498 | 6 | 4,08 | 256,766 |
| CH2 | 1 | 0,2293 | 19,8711 | 6 | 4,88 | 473,389 |

*Table 6- $\epsilon_{kl,}$ estimated from experimental data, and $\lambda^r_{kl,}$ obtained from equation 24, used within the SAFT-γ Mie group-contribution approach. In all cases the unlike diameters $\sigma_{kl}$ and $d_{kl}$ as well as the unlike attractive exponent of the Mie potential $\lambda_{kl}{}^{\alpha}$ are obtained from Equations 21, 22, and 24, respectively (Dufal, Papaioannou, Sadeqzadeh, & Pogiatzis, 2014).*

| Group k | Group l | $\epsilon_{kl}/kB$ (K) | $\lambda^r_{lk}$ |
|---|---|---|---|
| CH3 | H2O | 274,80 | 16,01 |
| CH2 | H2O | 284,53 | 18,39 |
| CH2 | CH3 | 350,77 | 17,26 |

*Table 7- Group association energy $\epsilon^{HB}{}_{kl,ab}$ and bonding volume parameter $K_{kl,ab}$ used within the SAFT-γ Mie group-contribution approach. (Dufal, Papaioannou, Sadeqzadeh, & Pogiatzis, 2014)*

| Group k | Site a of group k | Group l | Site b of group l | $\epsilon_{kk}/k_B$ (K) | $K_{kl,ab}$[Å $^3$] |
|---|---|---|---|---|---|
| H20 | H | H20 | e1 | 1985,4 | 101,7 |

## Results

The results obtained using the SAFT-γ-Mie theory are presented in figures 13 to 16.In the following figures, besides the experimental data from (Morgado, 2011), the data from (Maczynski A. , Shaw, Goral, & Wisniewska-Goclowska, 2005) was also included. The results were obtained recurring to the HELD algorithm, used to calculate the equilibrium phases.

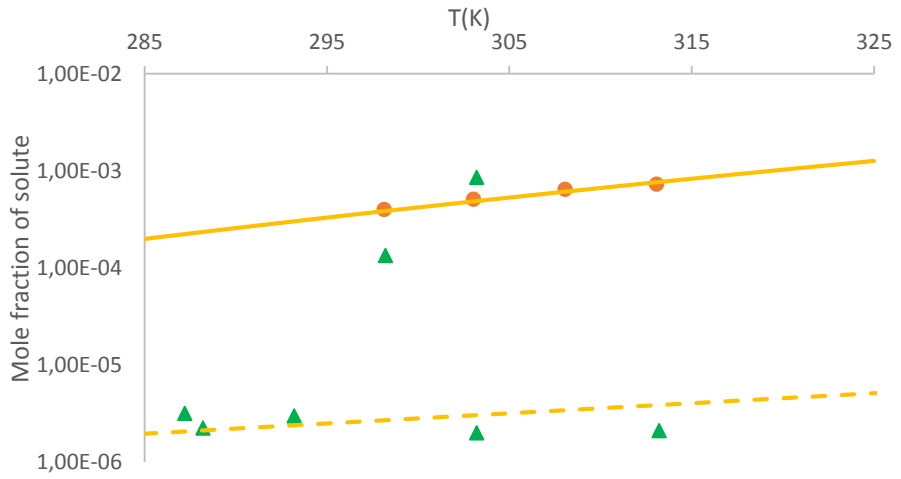


*Figure 13- Mole fraction of water in n-hexane (solid line) and of n-hexane in water (dotted line) as a function of temperature; triangles represent experimental data from (Maczynski A. , Shaw, Goral, & Wisniewska-Goclowska, 2005); filled circles represent experimental data from (Morgado, 2011); yellow line represents SAFT- γ-Mie predictions (tab 5, 6 and 7)*

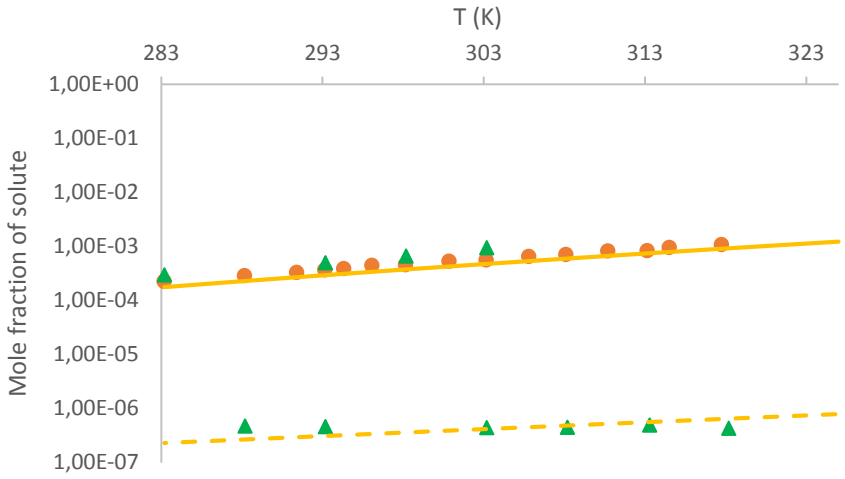


*Figure 14- Mole fraction of water in n-heptane (solid line) and of n-heptane in water (dotted line) as a function of temperature; triangles represent experimental data from (Maczynski A. , Shaw, Goral, & Wisniewska-Goclowska, 2005); filled circles represent experimental data from (Morgado, 2011); yellow line represents SAFT- γ-Mie results (tab 5, 6 and 7)*

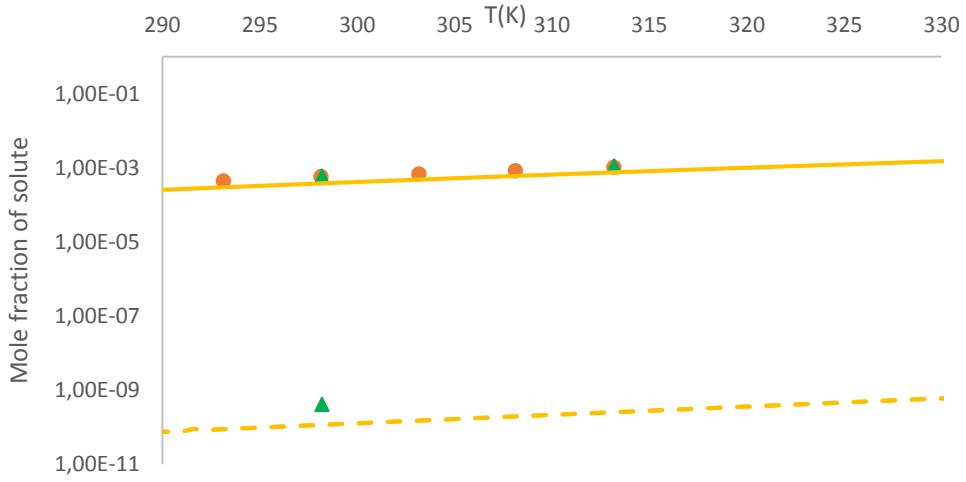


*Figure 15- Mole fraction of water in n-undecane (solid line) and of n-undecane in water (dotted line) as a function of temperature; triangles represent experimental data from (Maczynski A. , Shaw, Goral, & Wisniewska-Goclowska, 2005); filled circles represent experimental data from (Morgado, 2011); yellow line represents SAFT- γ-Mie predictions (tab 5, 6 and 7)*

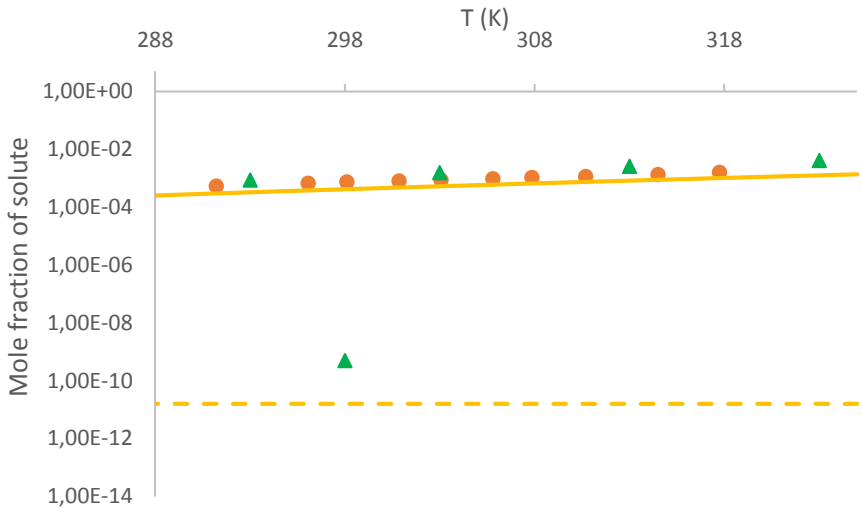


*Figure 16- Mole fraction of water in n-hexadecane (solid line) and of hexadecane in water (dotted line) as a function of temperature; triangles represent experimental data from (Maczynski A. , Shaw, Goral, & Wisniewska-Goclowska, 2005); filled circles represent experimental data from (Morgado, 2011); yellow line represents SAFT- γ-Mie predictions (tab 5, 6 and 7)*

As can be observed for all systems, the SAFT- γ-Mie solubility line follows thoroughly the solubility data in the oil rich phase. The water rich phase predictions aren't as accurate as the oil-rich phase, showing differences of one order of magnitude. However, this can be considered a relatively good prediction, taking into account that the absolute solubility values on this phase are extremely low.

# Chapter 4

## Thermodynamic Functions

In order to understand the behavior of water in the oil rich phase it is important to study the main thermodynamic properties of the various systems. The main standard thermodynamic functions of solution can be calculated from the temperature dependence of the experimental solubility data. For that purpose, the previously presented solubility results, both those obtained experimentally and with the two approaches of SAFT, were used. In this section the main thermodynamic properties will be calculated, such as the standard enthalpy of solution, $\Delta_{sol}H_m^0$, and the standard entropy of solution, $\Delta_{sol}S_m^0$.

For the process of transferring one mole of solute molecules from the pure liquid solute to a dilute ideal solution where the mole fraction of solute is equal to 1, the apparent standard molar Gibbs energy of solution at constant pressure for an ideal mixture is given by the following equation.

$$\Delta_{\mathrm{sol}}\mathrm{G}_{\mathrm{m}}^{0}(\mathrm{P},\mathrm{T},\mathrm{x}_{\mathrm{i}}) = -\mathrm{RT}\ln \mathrm{x}_{\mathrm{i}} \tag{30}$$

Assuming that the $\Delta_{sol}H_m^0$ and $\Delta_{sol}S_m^0$ are temperature independent and that the dissolution process takes place at constant temperature and pressure, the following relation is valid,

$$\Delta_{sol}G_m^0(P,T,x_i) = \Delta_{sol}H_m^0 - T\Delta_{sol}S_m^0 \tag{31}$$

Relating equations 30 and 31 one can use the following equation to obtain $\Delta_{sol}H_m^0$ and $\Delta_{sol}S_m^0$, from the temperature dependence of the solubility ($\Delta_{sol}H_m^0$ is the slope and the $\Delta_{sol}S_m^0$ is the intercept)

$$\ln \mathrm{x}_1 = -\frac{\Delta_{\mathrm{sol}}\mathrm{H}_{\mathrm{m}}^{0}}{\mathrm{RT}} + \frac{\Delta_{\mathrm{sol}}\mathrm{S}_{\mathrm{m}}^{0}}{\mathrm{R}} \tag{32}$$

For real solutions equation 30 should be expressed in terms of the activity coefficient of the solute, $\gamma_i$.

$$\Delta_{\mathrm{sol}}\mathrm{G}_{\mathrm{m}}^{0}(\mathrm{P},\mathrm{T},\mathrm{x}_{\mathrm{i}}) = -\mathrm{RT}\ln \gamma_i \mathrm{x}_{\mathrm{i}} \tag{33}$$

However, for very dilute solutions it is known that the change of $\gamma_i$ with composition becomes negligible. Thus, the enthalpy of solution, which is essentially the temperature derivative of the activity, becomes independent of the activity coefficient and equation 32 can be used to calculate $\Delta_{sol}H_m^0$ and $\Delta_{sol}S_m^0$.

Since the main goal of this work is to understand the solute-solvent interactions, it is useful to consider, instead of the dissolution process, the solvation process, in which the energies associated with extracting the solute molecules from the liquid solute are not considered. To obtain the standard molar enthalpy of solvation, $\Delta_{svt}H_m^0$, one can just subtract the molar enthalpy of vaporization of the solute, $\Delta_l^g H_m^0$ , (which is the enthalpy needed to bring the solute molecules from the liquid to the ideal gas state), from the standard enthalpy of solution, $\Delta_{sol}H_m^0$. Similarly, the standard molar entropy of solvation, $\Delta_{svt}S_m^0$ was obtained subtracting the molar entropy of vaporization, $\Delta_l^g S_m^0$ from the standard entropy of solution, $\Delta_{sol}S_m^0$.

## Results

As previously explained, standard enthalpies of solution, $\Delta_{sol}H_m^0$, and standard entropies of solution, $\Delta_{sol}S_m^0$, of water in all the n-alkanes studied, were calculated from the temperature dependence of both the experimental and theoretical solubility, recurring to equation 32. Standard molar quantities of solvation were also calculated. The molar enthalpy and entropy of vaporization, and the vapor pressure of water at 298.15 K were taken as 43,99 kJ.mol$^{-1}$ , 118,8 J.K$^{-1}$.mol$^{-1}$ , and 3,170 kPa, respectively (Morgado, 2011). The results are reported in tables 8 and 9, and plotted in the figure 17.

Table 8 - Standard molar enthalpies and entropies of solution, $\Delta_{sol}H_m^0$ and $\Delta_{sol}S_m^0$ at 298,15 K, from experiment, SAFT-VR-SW and SAFT-γ-Mie.

| | **Experimental** | | **SAFT-VR-SW ($K_{ij}$=opt)** | | **SAFT- γ -Mie** | |
|---|---|---|---|---|---|---|
| **System** | $\Delta_{sol}$H$^0$ (kJ/mol) | $\Delta_{sol}$ΔS$^0$ (J/mol) | $\Delta_{sol}$H$^0$ (kJ/mol) | $\Delta_{sol}$ΔS$^0$ (J/mol) | $\Delta_{sol}$H$^0$ (kJ/mol) | $\Delta_{sol}$ΔS$^0$ (J/mol) |
| **Water/n-hexane** | 32,7 | 44,5 | 36,5 | 57,1 | 37,0 | 56,5 |
| **Water/n-heptane** | 33 | 46,8 | 35,8 | 56,1 | 35,5 | 53,5 |
| **Water/n-undecane** | 30,6 | 40,5 | 35,4 | 56,2 | 35,3 | 52,9 |
| **Water/n-hexadecane** | 29,9 | 40,1 | 34,9 | 56,6 | 35,2 | 53,4 |

Table 9 - Standard molar enthalpies and entropies of solvation, $\Delta_{svt}H_m^0$ and $\Delta_{svt}S_m^0$ at 298,15 K, from experiment, SAFT-VR-SW and SAFT-γ-Mie.

| | **Experimental** | | **SAFT-VR-SW ($K_{ij}$=opt)** | | **SAFT- γ -Mie** | |
|---|---|---|---|---|---|---|
| **System** | $\Delta_{svt}$H$^0$ (kJ/mol) | $\Delta_{svt}$ΔS$^0$ (J/mol) | $\Delta_{svt}$H$^0$ (kJ/mol) | $\Delta_{svt}$ΔS$^0$ (J/mol) | $\Delta_{svt}$H$^0$ (kJ/mol) | $\Delta_{svt}$ΔS$^0$ (J/mol) |
| **Water/n-hexane** | -11,3 | -74,3 | -7,5 | -61,6 | -7,0 | -62,3 |
| **Water/n-heptane** | -11,0 | -72,1 | -8,2 | -62,7 | -8,5 | -65,3 |
| **Water/n-undecane** | -13,4 | -78,3 | -9,6 | -62,9 | -8,4 | -64,9 |
| **Water/n-hexadecane** | -14,1 | -78,7 | -8,9 | -60,8 | -8,8 | -65,4 |

As can be observed, the solution enthalpies are all positive, reflecting the energy required to separate the water molecules in liquid water before solubilizing in the alkane solvent. This energy can be taken as the molar enthalpy of vaporization. Once subtracted from the solution enthalpies, we obtain the solvation enthalpies, which are all negative. Both the experimental $\Delta_{sol}H_m^0$ and $\Delta_{sol}S_m^0$ seem to slightly decrease with the alkane chain length, but almost within experimental accuracy. One of the main purposes of this work is to obtain SAFT predictions for the solution/solvation enthalpies and to check if these depend on the alkane chain length, providing physical insight to the reasons of this dependence.

As can be seen from the theoretical results, the thermodynamic functions obtained from both SAFT-VR-SW and the SAFT-γ-Mie are essentially constant, although also slightly decreasing with the alkane chain length. It should be realized, however, that in both cases, binary interaction parameters were fitted to the experimental results. It is thus not surprising that the theoretical results reproduce the description of the solubility lines presented in the previous chapters. It might be argued that in the case of SAFT-γ-Mie, since the binary interaction parameter are defined and fitted for each functional group, CH2 and CH3, the theoretical predictions could reflect the influence of the alkane chain length.

## SAFT-VR-SW with an average $k_{ij}$

Since the results from tables 8 and 9 were obtain with optimized parameters for each system, and in order to grasp the variation of the thermodynamic properties with the chain length of the n-alkane chemical family, a different strategy was used. The SAFT-VR-SW equation was used to obtain theoretical predictions for a series of water/n-alkane binary systems, from n-Hexane to n-Hexadecane, but a single average binary interaction parameter was used, $k_{ij}$=0,29. For the sake of consistency, the pure component's parameters were obtained from correlations with the molar weight, equations 34 to 37 (Paricaud, Jackson, & Galindo, 2004).

$$m = 0{,}02376.MW(g.mol^{-1}) + 0{,}6188 \quad (34)$$

$$m.\lambda = 0{,}04024.MW(g.mol^{-1}) + 0{,}6570 \quad (35)$$

$$m.\sigma(\text{Å})^3 = 1{,}53212.MW(g.mol^{-1}) + 30{,}753 \quad (36)$$

$$m.(\frac{\epsilon}{k}) = 5{,}46587.MW(g.mol^{-1}) + 194{,}263 \quad (37)$$

The obtained SAFT-VR-SW parameters for each n-alkane are displayed in the following table 10.

*Table 10- SAFT-VR-SW parameters for each n-alkane obtained through equations, 34 to 37.*

| | SAFT-VR-SW $K_{ij}$=0,29 | | | | | |
|---|---|---|---|---|---|---|
| | **n-hexane** | **n-Octane** | **n-Decane** | **n-Dodecane** | **n-Tetradecane** | **n-hexadecane** |
| **m** | 2,7 | 3,3 | 4,0 | 4,7 | 5,3 | 6,0 |
| **MW** | 86,2 | 114,2 | 142,3 | 170,3 | 198,4 | 226,4 |
| $\boldsymbol{\lambda}$ | 1,6 | 1,6 | 1,6 | 1,6 | 1,6 | 1,6 |
| $\boldsymbol{\sigma}$ (Å) | 3,9 | 3,9 | 3,9 | 3,9 | 3,9 | 3,9 |
| $\boldsymbol{\epsilon}/\boldsymbol{k}$(K) | 249,5 | 245,6 | 243,0 | 241,1 | 239,8 | 238,7 |

Equation 32 was used to calculate the thermodynamic properties, $\Delta_{sol}H^0$ and $\Delta_{sol}S^0$. The standard enthalpy of solvation, was obtained, once again, subtracting the molar enthalpy of vaporization to the standard enthalpy of solution, while the entropy of solvation was calculated subtracting the molar entropy of vaporization to the standard entropy of solution, as explained previously.

*Table 11- SAFT-VR-SW results of $\Delta_{sol}H^0$ (kJ/mol), $\Delta_{sol}S^0$, $\Delta_{svt}H_m^0$ and $\Delta_{svt}S_m^0$ with an average $k_{ij}$ of 0,29, at 298,15 K.*

| | SAFT-VR-SW $K_{ij}$=0,29 | | | |
|---|---|---|---|---|
| **System** | $\Delta_{sol}H^0$ (kJ/mol) | $\Delta_{sol}S^0$ (J/mol) | $\Delta_{svt}H^0$ (kJ/mol) | $\Delta_{svt}S^0$ (J/mol) |
| **Water/n-hexane** | 36,5 | 57,1 | -7,5 | -61,7 |
| **Water/n-octane** | 35,5 | 56,0 | -8,5 | -62,8 |
| **Water/n-decane** | 35,1 | 56,0 | -8,8 | -62,8 |
| **Water/n-dodecane** | 34,9 | 56,3 | -9,1 | -62,5 |
| **Water/n-tetradecane** | 34,7 | 56,7 | -9,3 | -62,1 |
| **Water/n-hexadecane** | 34,6 | 57,1 | -9,4 | -61,7 |

The results in table 11 show the same decreasing tendency, although more gradual, of the thermodynamic properties, $\Delta_{sol}H^0$ and $\Delta_{sol}S^0$, with the n-alkane chain length than those observed in tables 8 and 9. Figure 17 summarizes the results from tables 8 and 11.

From figure 17 it is clear that, as a whole, the experimental values (orange) evidence a more acute decrease of the $\Delta_{sol}H^0$ with the n-alkane chain length. The SAFT-VR-SW results, with an optimized $k_{ij}$ for each system (blue dots) or with an average $k_{ij}$ both (yellow dots), predict approximately the same decrease of the thermodynamic property with the n-alkane chain length, and the results obtained throughout SAFT- γ –Mie (grey dots) evidence a less acute decrease.

In brief, the different theoretical predictions are very similar and they are able to reproduce the experimental trend although with an absolute difference of about 4-5 $J.mol^{-1}$.

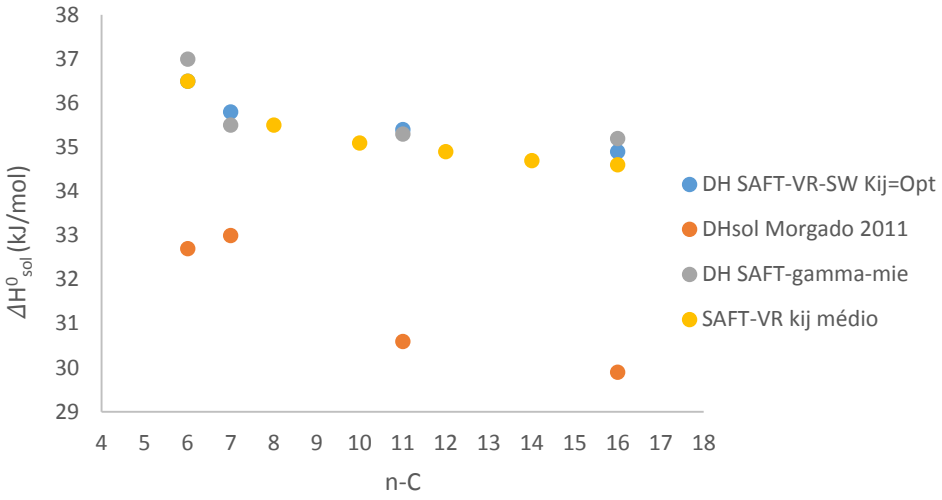


*Figure 17-Variation of the $\Delta H^0_{sol}$ (kJ/mol) results, tables 8 and 11, with the carbon number of the n-alkane, with all studied treatments. Calculated $\Delta H^0_{sol}$ (kJ/mol) obtained with: SAFT- γ –Mie (grey dots); SAFT-VR-SW with the $k_{ij}$ value adjusted to the oil rich phase (blue dots); SAFT-VR-SW with an average $k_{ij}$ (yellow dots); Experimental results from (Morgado, 2011) (orange dots).*

## Thermodynamic properties and the size of the solvent

Although the nature of all analyzed systems is very similar (water/n-alkane mixtures), the mixtures were studied within the same temperature range, thus at different reduced temperatures rages, therefore at different thermodynamic states. In figure 18 the enthalpy of solvation for all systems was plotted as a function of the average reduced temperature.

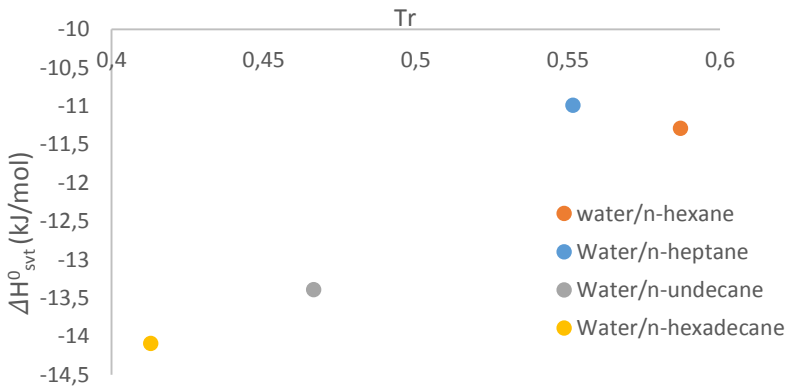


*Figure 18-Standard enthalpy of solvation, $H^0_{svt}$, for each binary system at its reduced temperature*

One can observe that although the $\Delta_{svt}H^0$ is larger (more negative) for the water/n-hexadecane mixture, its reduced temperature is also the lowest and hence the solvent is denser. In order to better compare the thermodynamic properties in terms of the water/n-alkane interaction, the system's properties should be compared at the same reduced temperature. However, this is not

easy as solubility data is scarce at higher temperatures. Figure 17 thus shows that the decrease of $\Delta_{svt}H^0$, is a result not only of the increase of the chain length of the alkane but also of the decrease of the reduced temperature of the solvent.

In figure 19, the same solubility data of water in all the studied n-alkanes is now expressed in molarity units (moles of solute per litter of solution) instead of mole fraction. As can be seen, the water solubility decreases with the chain length of the n-alkane and increases with temperature, being the mixtures with the highest molarity the water/n-hexane and water/n-heptane. These results seam to contradict those found in previous graphics where solubility was expressed in molar fraction of solute. When the solubility of water is expressed in molar fraction of water, the solubility increases with the chain length of the solvent, being water more soluble in n-hexadecane. This apparent contradiction obviously results from the different molecular size along the n-alkane series (The number of molecules in one liter of n-hexane is higher than the number of molecules of n-hexadecane in the same volume, since one molecule of hexadecane occupies a larger volume), but illustrates how important it is to make a proper choice of the solubility units depending of the effect that is being studied.

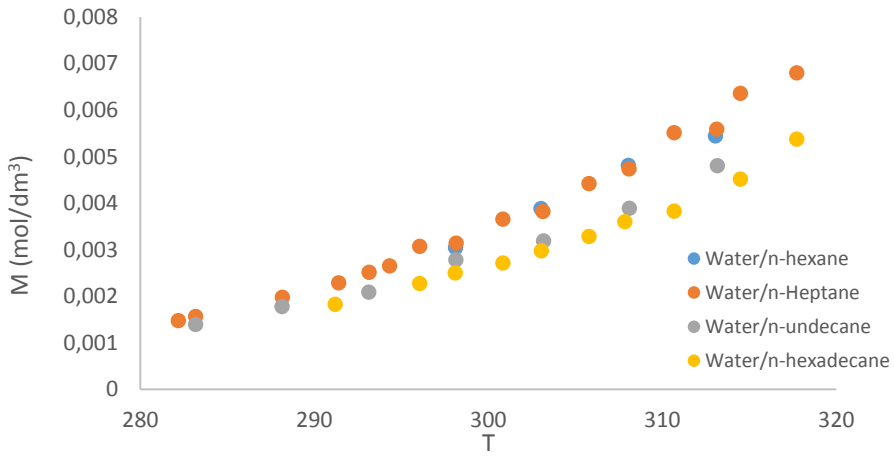


*Figure 19- Solubility data at different temperatures of experimental values of (Morgado, 2011) expressed in molarity for each solvent.*

# Chapter 5

## Conclusions

The main conclusions of this work can be summarised as follows:

1- It was found that the binary interaction parameter, $k_{ij}$, of the SAFT-VR-SW theory, can be adjusted to reproduce very accurately the oil rich phase of water/n-alkane mixtures from n-hexane to n-hexadecane, and the optimal value to reproduce these systems is very similar and within the rage of 0,30 to 0,28. It was also found that fitting the $k_{ij}$ to the oil rich phase lowers the solubility on both phases, allowing for a better description of the oil rich phase but underpredicting the water rich phase solubility curve. Hence the results with a fitted $k_{ij}$ for the oil rich phase mean a much more accurate description of the water/n-alkane system on that phase, but a much worse description of the water rich phase.

2- SAFT- γ –Mie theory was proven to present the best prediction of the solubility of water/n-alkane systems, with both phases accurately reproduced. Another important conclusion that can be established is that the model can reproduce more accurately the oil rich phase than the water rich phase.

3- The results also show that the thermodynamic functions both obtained from the experimental data and predicted by both versions of SAFT, decrease with the chain length of the alkane. The decrease predicted by the theory is less pronounced than that found experimentally and deviates from the experimental values by 5 $J.mol^{-1}$. The predictions of all theoretical treatments are very equivalent.

4- Although it was found that the best description of the experimental data for the oil-rich phase is given by SAFT-VR-SW with a fitted $k_{ij}$, not enough water/n-alkanes were studied to permit the elaboration of a correlation between the chain length and the $k_{ij}$ values. SAFT-VR-GC approach could have also been used, since it is a version of SAFT that uses a group contribution within the VR approach, and its results would have given and interesting overview on the development of the SAFT theory and how it predicts the water behavior on the oil rich phase, on water/n-alkanes binary systems.

5- It is hard to find an approach that it is able to reproduce both phases of the of water/n-alkane systems, since the interactions between the same components on the distinct phases are completely different. In the future, a wider range of temperature should be considered, and more water/n-alkane systems included.

6- The thermodynamic functions of the water/n-alkane systems should be obtained at the same reduced temperature, in order to understand how the solvents behave when in the same thermodynamic state. The enthalpy of interaction should also be studied to broaden the understanding of the water/n-alkane interaction on the oil-rich phase.

# Appendix A

## Tables of experimental data

*Table A1-Experimental solubility of water in the alkane rich phase at different temperatures, (Morgado, 2011).*

| System | T(K) | $x_{1B}$ | M(mol/dm$^3$) |
|---|---|---|---|
| **Water/n-Hexane** | 298,13 | 4,00E-04 | 0,0031 |
| | 303,03 | 5,10E-04 | 0,0039 |
| | 308,05 | 6,43E-04 | 0,0048 |
| | 313,06 | 7,30E-04 | 0,0054 |
| | | | |
| **Water/n-Heptane** | 282,18 | 2,13E-04 | 0,0015 |
| | 283,18 | 2,27E-04 | 0,0016 |
| | 288,16 | 2,89E-04 | 0,0020 |
| | 291,40 | 3,34E-04 | 0,0023 |
| | 293,16 | 3,70E-04 | 0,0025 |
| | 294,33 | 3,90E-04 | 0,0027 |
| | 296,06 | 4,50E-04 | 0,0031 |
| | 298,15 | 4,60E-04 | 0,0031 |
| | 300,85 | 5,40E-04 | 0,0037 |
| | 303,15 | 5,70E-04 | 0,0038 |
| | 305,80 | 6,58E-04 | 0,0044 |
| | 308,10 | 7,10E-04 | 0,0047 |
| | 310,69 | 8,30E-04 | 0,0055 |
| | 313,14 | 8,40E-04 | 0,0056 |
| | 314,50 | 9,60E-04 | 0,0064 |
| | 317,74 | 1,09E-03 | 0,0068 |
| | | | |
| **Water/n-Undecane** | 283,18 | 2,92E-04 | 0,0014 |
| | 288,14 | 3,70E-04 | 0,0018 |
| | 293,14 | 4,40E-04 | 0,0021 |
| | 298,14 | 5,90E-04 | 0,0028 |
| | 303,18 | 6,80E-04 | 0,0032 |
| | 308,12 | 8,30E-04 | 0,0039 |
| | 313,18 | 1,04E-03 | 0,0048 |
| | | | |
| **Water/n-Hexadecane** | 291,21 | 0,000535 | 0,0018 |
| | 296,06 | 0,000669 | 0,0023 |
| | 298,10 | 0,00074 | 0,0025 |
| | 300,85 | 0,0008 | 0,0027 |
| | 303,06 | 0,00088 | 0,0030 |
| | 305,80 | 0,00097 | 0,0033 |
| | 307,86 | 0,00107 | 0,0036 |
| | 310,69 | 0,00114 | 0,0038 |
| | 314,50 | 0,00135 | 0,0045 |

| | | | |
|---|---|---|---|
| | 317,74 | 0,00161 | 0,0054 |

*Table A2- Experimental solubility of water in the n-alkane rich phase ( $x_{1B}$) and solubility of the n-alkane in the water rich phase ( $x_{2A}$ ) at different temperatures, (Maczynski A. , Shaw, Goral, & Wisniewska-Goclowska, 2005), (Maczynski, Shaw, & Goral, 2004), (Wisniewska-Goclowska, Shaw, Skrzecz, Góral, & Maczynski, 2003), (Shaw, Maczynski, & Goral, 2005), (Shaw, Maczynski, & Goral, 2006).*

| System | IUPAC-NIST | | | |
|---|---|---|---|---|
| | T(K) | $x_{1B}$ | T(K) | $x_{2A}$ |
| **Water/n-hexane** | 273,2 | 1,34E-04 | 273,2 | 3,44E-06 |
| | 298,2 | 4,30E-04 | 277,2 | 3,42E-06 |
| | 303,2 | 8,56E-04 | 287,2 | 3,17E-06 |
| | 354,8 | 6,70E-03 | 288,2 | 2,24E-06 |
| | 366,5 | 1,00E-02 | 293,2 | 3,00E-06 |
| | 379,3 | 1,51E-02 | 303,2 | 2,00E-06 |
| | 394,3 | 2,30E-02 | 313,2 | 2,11E-06 |
| | 400,4 | 2,72E-02 | 328,9 | 2,76E-06 |
| | 417,6 | 4,21E-02 | 342,9 | 3,18E-06 |
| | 422 | 4,74E-02 | 372,2 | 4,68E-06 |
| | 431,5 | 5,75E-02 | 387,5 | 6,10E-06 |
| | 442,6 | 7,30E-02 | 394,5 | 7,86E-06 |
| | 449,8 | 8,44E-02 | 410,5 | 1,19E-05 |
| | 452,6 | 9,02E-02 | 425 | 2,32E-05 |
| | 460,4 | 1,03E-01 | | |
| | 468,2 | 1,29E-01 | | |
| | 477,6 | 1,40E-01 | | |
| **Water/n-heptane** | 273,2 | 1,50E-04 | 273,2 | 7,88E-07 |
| | 283,2 | 3,00E-04 | 288,2 | 4,80E-07 |
| | 293,2 | 5,00E-04 | 293,2 | 4,62E-07 |
| | 298,2 | 6,70E-04 | 303,2 | 4,47E-07 |
| | 303,2 | 9,57E-04 | 308,2 | 4,53E-07 |
| | 313,2 | 8,70E-04 | 313,3 | 5,00E-07 |
| | | | 318,2 | 4,32E-07 |
| | | | 328,9 | 5,60E-07 |
| | | | 372,3 | 1,01E-06 |
| | | | 391,2 | 2,05E-06 |
| | | | 409,8 | 4,91E-06 |
| | | | 423,6 | 7,86E-06 |
| **Water/n-undecane** | 298,2 | 6,00E-04 | 298,2 | 4,1E-10 |
| | 313,2 | 1,13E-03 | | |
| **Water/n-hexadecane** | 293 | 8,67E-04 | 298 | 5E-10 |
| | 303 | 1,55E-03 | | |
| | 313 | 2,62E-03 | | |
| | 323 | 4,16E-03 | | |

# Appendix B

*Table B1-Critical temperature, $T_C$, considered for each system and calculated relative temperature, $T_r$, for the experimental data of (Morgado, 2011).*

| | $T_c$ (K) | $T_r$ |
|---|---|---|
| **Water/n-Hexane** | 507,7 | 0,59 |
| | | 0,60 |
| | | 0,61 |
| | | 0,62 |
| **Water/n-Heptane** | 540,2 | 0,52 |
| | | 0,52 |
| | | 0,53 |
| | | 0,54 |
| | | 0,54 |
| | | 0,54 |
| | | 0,55 |
| | | 0,55 |
| | | 0,56 |
| | | 0,56 |
| | | 0,57 |
| | | 0,57 |
| | | 0,58 |
| | | 0,58 |
| | | 0,58 |
| | | 0,59 |
| **Water/n-Undecane** | 639 | 0,44 |
| | | 0,45 |
| | | 0,46 |
| | | 0,47 |
| | | 0,47 |
| | | 0,48 |
| | | 0,49 |
| **Water/n-Hexadecane** | 722 | 0,40 |
| | | 0,41 |
| | | 0,41 |
| | | 0,42 |
| | | 0,42 |
| | | 0,42 |
| | | 0,43 |
| | | 0,43 |
| | | 0,44 |
| | | 0,44 |

# Bibliography


Banaszak, M., Chiew, Y. C., & Radosz,, M. (1993). *Phys. Rev. E 48*.

Blas, F. J., & Vega, L. F. (1997). *Mol. Phys.* , 35.

Blas, F. J., & Vega, L. F. (1998). Prediction of Binary and Ternary Diagrams Using the Statistical Associating Fluid Theory (SAFT) Equation of State. *Ind. Eng. Chem. Res.*, 660-674.

Boublík, T. (1971). *Journal of Chemical Physics 54*.

Chapman, W. G., Gubbins, K. E., Jackson, J., & Radosz, M. (1989). *Fluid Phase Equilibria 52*.

Chapman, W. G., Jackson, G., & Gubbins, K. E. (1988). *Molecular Physics 65*.

Clark, G., Haslam, A., Galindo, A., & Jackson, G. (2006). Developing optimal Wertheim-like models of water for use in Statistical Associating Fluid Theory (SAFT) and related approaches. *Molecular Physics Vol. 104 No. 22-24*, pp. 3561-3581.

Dufal, S., Papaioannou, V., Sadeqzadeh, M., & Pogiatzis, T. (2014). Prediction of thermodynamic properties and phase behaviour of fluids and mixtures with the SAFT-γ Mie group contribution equation of state.

Economou, I. G., & Tsonopoulos, C. (1997). Associating models and mixing rules in equations of state for water/hydrocarbon mixtures. *Chemical Engineerino Science*.

Ferguson, A. L., Debenedetti, P. G., & Panagiotopoulos, A. Z. (2009). Solubility and Molecular Conformations of n-Alkane Chains in Water. *Journal of Physical Chemistry*.

Galindo, A., & McCabe, C. (2010). SAFT Associating Fluids and Fluid mixtures (Chap 8). In A. R. Goodwin, J. Sengers, & C. J. Peters, *Applied Thermodynamics of Fluids* (pp. 215-279).

Gil-Villegas, A., Galindo, A., Whitehead, P. J., Mills, S., Jackson, G., & Burgess, A. N. (1997). Statistical associating fluid theory for chain molecules with attractive potentials of variable range. *The Journal of Chemical Physics*, pp. 106, 4168–4186.

Gross, J., & Sadowski, G. (2001). *Ind. Eng. Chem. Res.*, 1244-1260.

Johnson, J. K., Muller, E. A., & Gubbins, E. K. (1994). *Journal of Physical Chemistry*.

Lafitte, T., Apostolakou,, A., Avendaño, C., Galindo, A., Adjiman, C. S., Müller, E. A., & Jackson, G. (2013). Accurate statistical associating fluid theory for chain molecules formed from Mie segments. *The Journal of Chemical Physics*.

Llóvell, F., Pàmies, J. C., & Vega, L. (2004). Thermodynamic properties of Lennard-Jones chain molecules: Renormalization-group. *The Journal of Chemical Pysics*.

Maczynski, A., Shaw, D. G., Goral, M., & Wisniewska-Goclowska. (2005). IUPAC-NIST Solubility Data Series. 81. Hydrocarbons with Water and SeawaterPart 4. C 6 H 14 Hydrocarbons with Water. *Journal of Physical and Chemical*.

Maczynski, A., Shaw, G. D., & Goral, M. (2004). IUPAC-NIST Solubility Data Series. 81. Hydrocarbons with Water and Seawater-Revised and Updated. Part 5. C 7 Hydrocarbons with Water and Heavy Water. *Journal of Physical and Chemical*.

Mansoori, G. A., Carnahan, N. F., Starling, K. E., & Leland, T. W. (1971). *Journal of Chemical Physics 54* .

Marche, C., Ferronato, C., & Jose, J. (2003). Solubilities of n-Alkanes (C6 to C8) in Water from 30 °C to 180 °C. *Journal of Chemistry*.

Marsh, K. N. (1987). Recommended Reference Materials for the Realization. Blackwell, Oxford.

McCabe, C., Galindo, A., GiI-Villegas, A., & Jackson, G. (1998). Predicting the High-Pressure Phase Equilibria of Binary Mixtures of n-Alkanes Using the SAFT-VR Approach. *International Journal of Therrnophysics*.

McCabe, C., Galindo, A., Gil-Villegas, A., & Jackson, G. (1998). Predicting the High-Pressure Phase Equilibria of Binary Mixtures of Perfluoro-n-alkanes +n-Alkanes Using the SAFT-VR Approach. *Journal of Physical Chemistry* .

Morgado, P. (2011). *Semifluorinated Alkanes – Structure – Properties Relations,PhD Thesis Pag 153-156.* Lisboa: IST Lisboa.

Morgado, P., Bonifácio, R., Martins, L. F., & Eduardo, F. J. (2013). *Probing the Structure of Liquids with 129Xe NMR Spectroscopy.* The Journal of Physical Chemistry.

Papaioannou, V., Lafitte, T., Avendaño, C., Adjiman, C. S., Jackson, G., Müller, E. A., & Galindo, A. (2014). Group contribution methodology based on the statistical associating fluid theory for heteronuclear molecules formed from Mie segments. *The Journal of Chemical Physics*.

Paricaud, P., Jackson, G., & Galindo, A. (2004). Modeling the Cloud Curves and the Solubility of Gases in Amorphous and Semicrystalline Polyethylene with the SAFT-VR and Approach and Flory Theory of Crystallization. *Ind. Eng. Chem. Res. Vol.43, No. 21*, pp. 6871-6889.

Patel, B., Galindo, A., Maitland, G., & Paricaud, P. (2003). Prediction of the Salting-Out Effect of Strong Electrolytes on Water + Alkane Solutions. *Ind. Eng. Chem. Res.*, 3-5.

Ramosa, M., Docherty, H., Blas, F. J., & Galindo, A. (2009). Application of the generalised SAFT-VR approach for long-ranged square-well potentials to model the phase behaviour of real fluids. *Fluid Phase Equilibria*, 116-126.

Rodrigues, D. E. (2012). *Molecular Modelling of Fluorinated compounds.*

Salvino, L. W., & White, J. A. (1992). *Journal of Chemical Physics*.

Shaw, D., Maczynski, A., & Goral, M. (2005). IUPAC-NIST Solubility Data Series. 81. Hydrocarbons with Water and Seawater—Revised and Updated. Part 10. C 11 and C 12 Hydrocarbons with Water. *Journal of Physical and Chemical*.

Shaw, D., Maczynski, A., & Goral, M. (2006). IUPAC-NIST Solubility Data Series. 81. Hydrocarbons with Water and Seawater—Revised and Updated. Part 11. C 13 – C 36 Hydrocarbons with Water. *Journal of Physical and Chemical*.

Tsonopoulos, C., & Wilson, G. M. (1983). *AIChE Journal*.

Vega, L. F., Llovell, F., & Blas, F. J. (2009). Capturing the Solubility Minima of n-Alkanes in Water by Soft-SAFT. *J. Phys. Chem.* , 7621–7630.

Wertheim, M. S. (1984). *J. Stat. Phys.* , 19-34.

Wisniewska-Goclowska, B., Shaw, D., Skrzecz, A., Góral, M., & Maczynski, A. (2003). Mutual Solubilities of Water and Alkanes. *Monatshefte fur Chemie*.